

Stochastic Modeling and Performance Analysis of Multi-tier HetNets



By

Anum Umer

Fall 2015-MS(EE)-7-00000118163

Supervisor

Dr. Syed Ali Hassan

Department of Electrical Engineering

A thesis submitted in partial fulfillment of the requirements for the degree
of Masters of Science in Electrical Engineering (MS EE)

In

School of Electrical Engineering and Computer Science,
National University of Sciences and Technology (NUST),

Islamabad, Pakistan.

(June 2017)

Approval

It is certified that the contents and form of the thesis entitled “**Stochastic Modeling and Performance Analysis of Multi-tier HetNets**” submitted by **Anum Umer** have been found satisfactory for the requirement of the degree.

Advisor: **Dr. Syed Ali Hassan**

Signature: _____

Date: _____

Committee Member 1: **Dr. Sajid Saleem**

Signature: _____

Date: _____

Committee Member 2: **Dr. Fahd Ahmed Khan**

Signature: _____

Date: _____

Committee Member 3: **Dr. Rizwan Ahmad**

Signature: _____

Date: _____

Abstract

The existing cellular systems operating in ultra high frequency bands suffer from severe bandwidth congestion and therefore, over the past few years, the paradigm of cellular spectrum is shifting towards millimeter wave (mmWave) bands under the umbrella of fifth generation (5G) networks to provide higher capacity. On the other hand, providing secure and reliable transmission of data to the desired users is gaining more importance in recent years. In this thesis, we analyze the impact of co-existence of mmWave small cells and massive multiple-input multiple-output (MIMO) on coverage and rate of the heterogeneous networks (HetNets). Specifically, we consider a three-tier network consisting of small cells operating at both the sub-6GHz and mmWave frequency bands overlaid with massive MIMO-enabled macro base stations. Based on the stochastic models, we investigate user association, coverage probability and data rate of the network. The proposed approach enhances the coverage performance of HetNets significantly. This model is further integrated with eavesdroppers under variable eavesdroppers density and antenna gains for the investigation of secrecy outage and connection outage. The user location of both the desired entities and eavesdroppers are modeled by independent Poisson point processes. Based on this stochastic model, we investigate the downlink secrecy outage probability, connection outage prob-

ability, area spectral efficiency (ASE) and energy efficiency (EE) of the entire network. The proposed approach of massive MIMO-enabled hybrid heterogeneous networks (HetNet) alongside mmWave small cells significantly reduces both the connection outage and secrecy outage probability and enhances achievable ASE and EE of the network for higher small cells base station density. Simulations are performed to validate the stochastic models.

Dedication

I dedicate this thesis to my most amazing parents and teachers.

Certificate of Originality

I hereby declare that this submission is my own work and to the best of my knowledge it contains no materials previously published or written by another person, nor material which to a substantial extent has been accepted for the award of any degree or diploma at NUST SEECS or at any other educational institute, except where due acknowledgement has been made in the thesis. Any contribution made to the research by others, with whom I have worked at NUST SEECS or elsewhere, is explicitly acknowledged in the thesis.

I also declare that the intellectual content of this thesis is the product of my own work, except for the assistance from others in the project's design and conception or in style, presentation and linguistics which has been acknowledged.

Author Name: **Anum Umer**

Signature: _____

Acknowledgment

I would like to thank Allah Almighty for bestowing me with His blessings of opportunity, determination and consistency to carry out this research work without which nothing could have become possible. I am immensely grateful for His kindness.

I would like to extend my sincere gratitude to my advisor, Dr. Syed Ali Hassan, for his constant support and consistency of advising me throughout this journey of research. I consider it a greatest opportunity and a blessing of Allah Almighty that I got to work under his supervision for if it was not him I would not have been able to come up with anything worthy of putting in the thesis. I am extremely grateful for his guidance at every single point and his attitude as an advisor serves as a role model for me.

Finally I would like to thank my most supportive, understanding and dedicated parents as without their encouragement and guidance I would not have been able to come this far. You are my backbone and your confidence in me makes me perform my best at every stage of life. Thank you

Table of Contents

1	Introduction	1
1.1	5G Networks	1
1.2	Thesis Contribution	2
1.3	Thesis Organization	3
2	Background and Literature Review	5
2.1	Heterogeneous Networks	5
2.2	Millimeter Wave Technology	7
2.3	Massive Multiple-Input Multiple-Output	8
3	5G Massive MIMO Hybrid HetNets Analysis	10
3.1	System Model	11
3.1.1	Downlink User Association	12
3.2	Channel Model	13
3.2.1	Blockage Model	15
3.3	Performance Analysis	15
3.3.1	Association Probability per Tier	16
3.3.2	Coverage Probability	18
3.3.3	Rate Coverage Probability	21
3.4	Simulation and Numerical Results	21

<i>TABLE OF CONTENTS</i>	viii
4 5G Green Hybrid HetNets Secrecy Analysis	27
4.1 System Model	28
4.1.1 Downlink User Association	29
4.1.2 Channel Model	29
4.1.3 Blockage Model	32
4.1.4 Area Spectral Efficiency and Energy Efficiency	32
4.2 Performance Analysis	33
4.2.1 Reliable and Secure Transmission Characterization	33
4.2.2 Association Probability	34
4.2.3 Connection Outage Probability	36
4.2.4 Secrecy Outage Probability	39
4.3 Simulation and Numerical Results	41
5 Conclusions and Future Works	50

List of Figures

1.1	A heterogeneous network	2
2.1	A HetNet with mmWave tier and massive MIMO at macro tier.	7
2.2	mmWave frequency spectrum.	8
2.3	massive MIMO antenna array.	9
3.1	Snapshot of a downlink three-tier heterogenous network. . . .	12
3.2	Association probability verses N with $\lambda_2 = \lambda_3 = 30\lambda_1$ and $S = 5$	22
3.3	SINR coverage probability $P_C(\Gamma)$ verses SINR threshold Γ for $N = 4$ and $S = 2$	23
3.4	SINR coverage probability $P_C(\Gamma)$ verses SINR threshold Γ for $N = 4$ and $S = 2$	24
3.5	Rate coverage probability R_C verses rate threshold ρ for $N = 4$ and $S = 2$	25
3.6	Rate coverage probability R_C^k verses rate threshold ρ for $\lambda_2 =$ $\lambda_3 = 30\lambda_1$, $N = 4$ and $S = 2$	26
4.1	Association probability verses varying relative small mmWave BS density λ_3/λ_1 for $\lambda_2 = 30\lambda_1$, $N = 100$ and $S = 5$	42

4.2	Secrecy outage probability verses Γ_e (dB) for $\lambda_2 = \lambda_3 = 30\lambda_1$, $N = 5$	43
4.3	Secrecy outage probability as the function of λ_e for $\Gamma_e = 40$ dB, $N = 5$	44
4.4	Secrecy outage probability verses Γ_e (dB) for $G_e = 15$ dB, $\lambda_2 =$ $\lambda_3 = 30\lambda_1$	45
4.5	EE verses SINR threshold Γ and rate coverage probability verses achievable rate in Mbps ρ for $N = 4$, $S = 2$, $\lambda_u =$ 1×10^{-4} , $\epsilon = 0.9$ and $\rho_c = 0.1$ W	46
4.6	Connection outage probability verses SINR threshold Γ (dB) for $N = 4$ and $S = 2$	47
4.7	EE and SE verses SINR threshold Γ (dB) for $N = 4$, $S = 2$, $\lambda_u = 1 \times 10^{-4}$, $\epsilon = 0.9$ and $\rho_c = 0.1$ W	48
4.8	Connection outage probability verses SINR threshold Γ for $N = 4$ and $S = 2$	49

Chapter 1

Introduction

This chapter presents an introduction about fifth generation (5G) technology. After that, thesis contribution followed by thesis organization concludes this chapter.

1.1 5G Networks

The world is rapidly moving towards its faster and smarter version of connectivity where not only humans but everything will be connected as a single network. Hereby, 5G will revolutionize the existing telecommunication standards of 4G networks to its new era of higher capacity, lower latency and ultra reliable wireless communication. In this thesis, we discuss the 5G enabling technologies such as heterogeneous networks (HetNets), millimeter wave (mmWave) technologies, massive multiple-input multiple-output (MIMO) technology and reliable and secure networks. The HetNets complement the conventional cellular network resources by an overlay deployment of low-powered base stations that creates a fusion of technologies, frequency

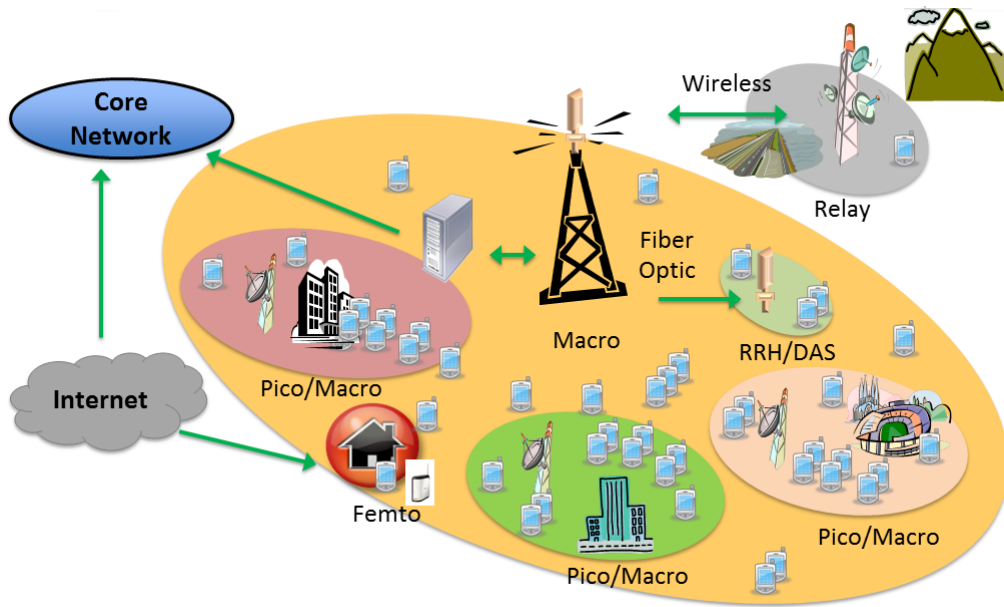


Figure 1.1: A heterogeneous network

bands, diverse cell sizes and network architectures that has a great ability to compensate for the drastic proliferation of wireless data traffic coverage and rate demands. The mmWave technology integration with microwave technology has paved a promising way for provision of higher data rates to the users. Massive MIMO integration on the microwave technology makes it capable of providing high gains and is thus seen as key enabler of 5G communication. This article proposes a framework to look into the possible advantages of these aforementioned technologies and provides an insight on their importance and challenges associated with them.

1.2 Thesis Contribution

Main contributions of this thesis can be listed as:

- This thesis presents a hybrid heterogeneous system model composed of multiple tiers operating at micro wave frequencies and mmWave frequencies. Massive MIMO is added at the macro tier. All tiers are modeled stochastically as Poisson Point Processes (PPP) with a certain density and a system model is developed.
- We study and stochastically model user association, coverage and rate trends of proposed network in the downlink transmission scenario. The proposed system model tend to have much better coverage and rate trends compared to traditional sub-6 GHz cellular networks without mmWave and massive MIMO technology.
- We propose a system model with legitimate users as well as eavesdroppers present in the multi-tier hybrid HetNet. Both the legitimate users and eavesdroppers are modeled as independent Poisson Point Processes.
- The secrecy outage probability and connection outage probability alongside energy efficiency (EE) and area spectral efficiency (ASE) are stochastically modeled and analyzed for this system model and it is observed that higher density of small cells leads to better secrecy outage probability and connection outage probability and system outperforms the traditional sub-6 GHz cellular networks.

1.3 Thesis Organization

The rest of the thesis is organized as follows: Chapter 2 outlines the background and existing literature on 5G wireless networks enabling technologies and highlights the advancements made in recent years. In Chapter 3, we

formulate the system model for multi-tier hybrid HetNet and look into the possible increment in coverage and rate of existing sub-6GHz cellular networks by addition of mmWave and massive MIMO technology. Chapter 5 presents the study of ASE and EE and the discussion on secrecy outage and connection outage on the proposed hybrid HetNet model in the presence of eavesdroppers. Chapter 6 concludes this article by discussing the conclusions drawn from the performance analysis of proposed system models followed by future works based on the proposed framework.

Chapter 2

Background and Literature Review

This chapter provides the background and discusses the capability of the key enabling technologies for the upcoming fifth generation mobile networks and their literature review. The key technologies for the 5G networks discussed in this chapter include multi-tier networks provided with small cells, higher frequency technology and massive Multiple- Input Multiple- Output technology.

2.1 Heterogeneous Networks

Over the years, the data rate demands have increased immensely owing to widespread usage of smart phones and wireless technologies [1]. The exponential growth in traffic calls for making use of higher frequency bands in addition to conventional cellular networks operating at sub-6GHz bands. The upcoming 5G technology is thought of, by researchers, as a mixture of

multiple network tiers of variable sizes, transmit powers, range and operating frequencies, making a HetNet. The HetNets complement the conventional cellular network resources by an overlay deployment of low-powered base stations that creates a fusion of technologies, frequency bands, diverse cell sizes and network architectures that has a great ability to compensate for the drastic proliferation of wireless data traffic coverage and rate demands [2,3]. Thus, the 5G technology can be visualized as a combination of a mixed HetNets that are modeled to enhance the network coverage area and data rates [4–6]. These advantage of HetNets come at the cost of user association, interference management for multiple tiers, hardware cost and deployment cost, energy efficiency, load balancing and many other [7–11,41–53].

A hybrid HetNets provided with multiple tiers and massive MIMO at macro tier is shown in Fig. 2.1. The HetNets provide high data rates and a lot of investigation into their various performance aspects has been performed by researchers. Authors in [12,13] analysed performance of mmWave hybrid networks based on simulation models. The authors in [14] investigated user association for massive MIMO HetNets and [15] stochastically modelled user association and coverage for K-tier HetNet with massive MIMO in macro tier. The energy efficiency and area spectral efficiency aspects of HetNets have been discussed in [16–18].

Whereas much emphasis is laid on connection and rate performance of these networks, a considerable work has been done on physical layer security implementation in HetNets. For instance, the secrecy capacity of unicast links in the presence of eavesdroppers where transmission to the desired node is based on distance is studied in [43]. Similarly, secrecy outage probability for wireless fading channel was investigated in [41] and [42].

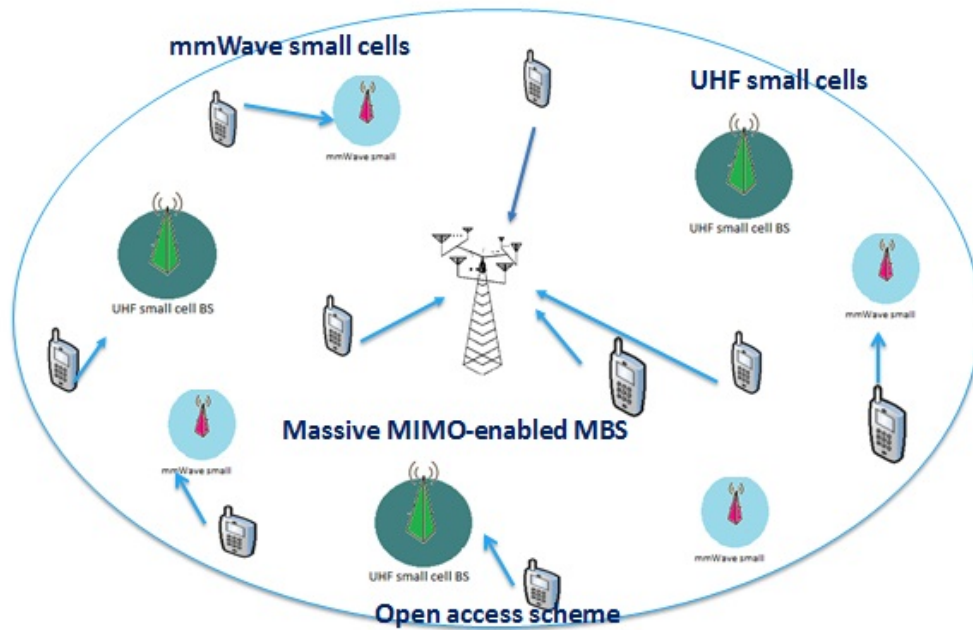


Figure 2.1: A HetNet with mmWave tier and massive MIMO at macro tier.

The stand alone sub-6GHz networks are not affected by blockages but mmWave communication is hindered and suffers propagation loss [22]. The authors in [23] have studied the secrecy and outage capacity under the effect of blockages for mmWave overlaid microwave network in the presence of eavesdroppers.

2.2 Millimeter Wave Technology

The exponential growth in traffic calls for making use of higher frequency bands in addition to conventional sub-6GHz bands. 5G promises wide range of applications alongside high data rates but existing cellular infrastructure works on sub-6GHz bands, which is unable to meet the 5G data demands. However, millimeter wave (mmWave) communication base stations (BSs)

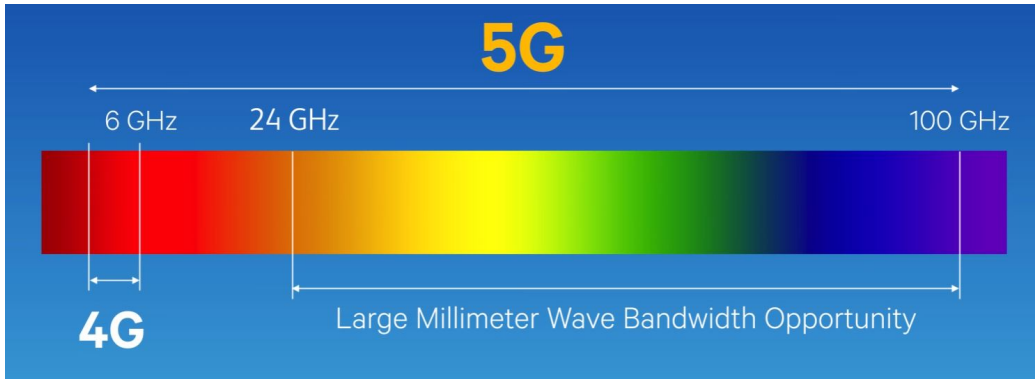


Figure 2.2: mmWave frequency spectrum.

operating at 10 to 300 GHz frequency bands with bandwidths up to 2 GHz rightfully serve the purpose [24–27, 39].

Though mmWave technology promises high data rates yet owing to its high frequency it has to deal with propagation losses, reflection losses and issues of line-of-sight (LOS) and non-line-of-sight (NLOS) transmission alongside hardware expenses [29]. However certain techniques such as beamforming and highly directional antennas tend to increase its range to around 150-200 meters. Formation of hybrid HetNets and co-existence of mmWave and microwave technology is seen as a key enabler for huge data traffic and high data rate demands [4, 27, 39].

2.3 Massive Multiple-Input Multiple-Output

Multiple antenna arrays at sub-6GHz base stations providing high array gains are seen as key enablers of 5G communication providing high coverage and data rates [24]. Each base station is provided with multiple antennas that serves multiple users simultaneously. Their high gains make it a favourable application at the existing sub-6 GHz base stations to make them support

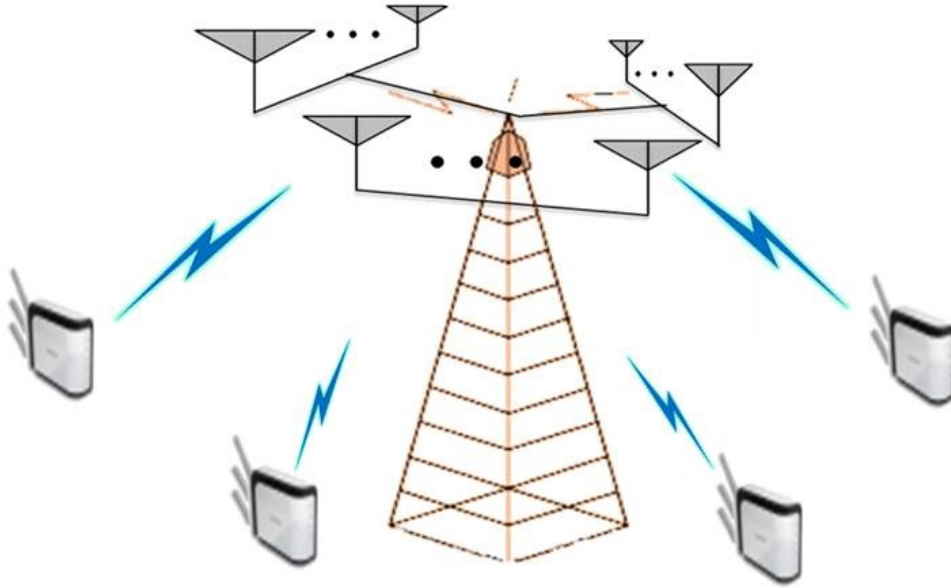


Figure 2.3: massive MIMO antenna array.

high data rates and energy efficiency.

Massive multiple-input multiple-output (MIMO) has gathered researchers attention and a lot of work is being done on their performance. For instance, User association with BSs in massive MIMO HetNets is investigated in [14] and the user association per tier and coverage probability for K-tier HetNets with massive MIMO in the macro tier is stochastically modeled in [15]. The massive MIMO has been investigated in [30], it presents results for achievable rate in uplink network scenario for MIMO at BSs. The impact of massive MIMO in interference mitigation has been presented by authors in [31] and its performance in spectrum sharing networks has been discussed in [38]. Performance analysis of massive MIMO technology with zero forcing beamforming (ZFBE) has been investigated in [33].

Chapter 3

5G Massive MIMO Hybrid HetNets Analysis

In this chapter, we present the stochastic geometry models for analysis of 3-tier network composed of massive MIMO enabled sub 6-GHz macro cells overlaid with mmWave and sub 6-GHz small cells. We analyse network performance in terms of user association, network coverage and data rate. To the best of our knowledge, no prior work has investigated network performance of mmWave small cells coexisting with traditional heterogeneous networks while assuming Nakagami fading model for mmWave communication and massive MIMO enabled macro BSs (MBSs). We deploy N antennas at each macro cell BS which simultaneously transmit data streams to S users using linear zero-forcing beamforming and mmWave and sub-6GHz small cells BS are deployed at higher density than MBSs and user association, coverage and rate trends are discussed.

3.1 System Model

We consider the downlink transmission scenario of a three-tier HetNet comprising of sub-6GHz macro cells overlaid with small cells operating at sub-6GHz and mmWave frequency band, as shown in Fig. 3.1. The BSs of k^{th} tier are uniformly distributed as Homogeneous Poisson Point Process (HPPP) Φ_k with density λ_k where $k = \{1, 2, 3\}$. The users are also assumed to be uniformly distributed as HPPP Φ_u with density λ_u . The sub-6GHz small cells constitute tier 2 while tier 3 constitutes small cells operating at mmWave frequency band. Massive MIMO is implemented at the macro cells where N antennas are installed at each MBS which simultaneously transmit to S users such that $N \gg S \geq 1$ [31]. The sub-6GHz small cell BSs, mmWave BSs and users are single antenna nodes. Zero forcing beamforming is used by each MBS for transmitting S data streams with equal power assignment. Transmission is taken to be time-division duplex (TDD) and it is assumed that downlink channel state information is known at the MBS [15]. Analysis is performed for a typical user located at the origin, in accordance with Slivnyak's Theorem. The mmWave small cells can have either line of sight (LoS) or Non-line of sight (NLoS) link to the typical user. To cater for this we split Φ_3 , by applying independent thinning theorem, to Φ_3^L and Φ_3^N as point processes of LoS and NLoS mmWave small cells, using LoS probability function $p(R)$, to evaluate that a link of length R is LoS or NLoS [22]. Thus, Φ_3^L and Φ_3^N have the densities $p(R)\lambda_3$ and $(1 - p(R))\lambda_3$, respectively, while $p(R)$ is discussed in detail in Section III.

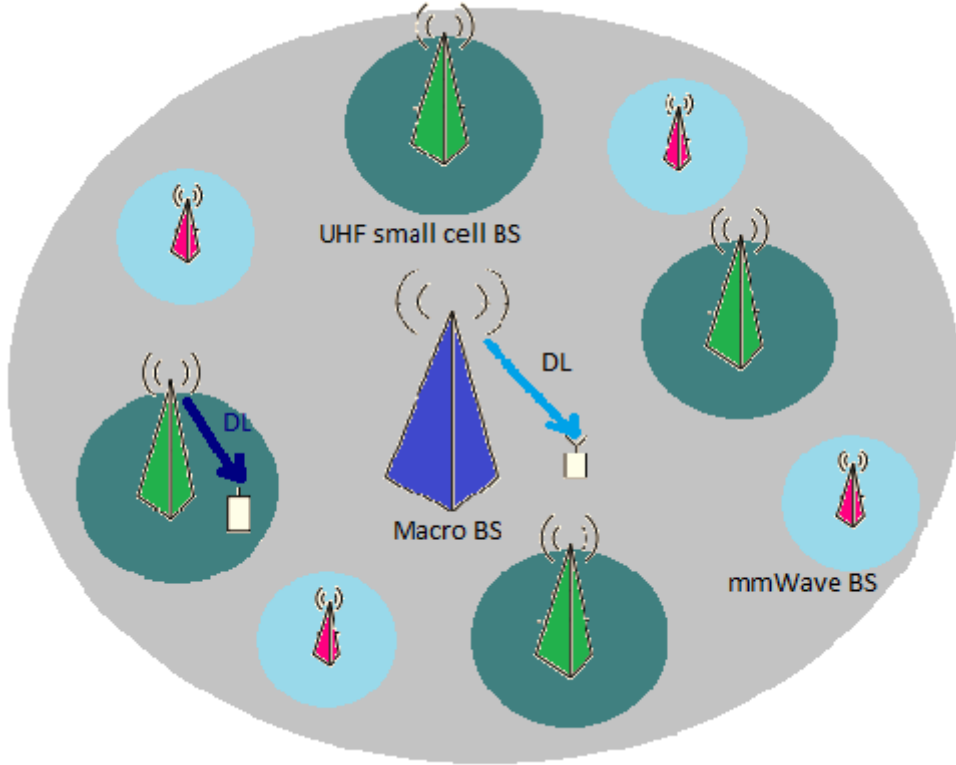


Figure 3.1: Snapshot of a downlink three-tier heterogenous network.

3.1.1 Downlink User Association

An open access scheme has been assumed such that user is allowed to connect to any tier BS. We assume user association is based on maximum average received power, i.e., a user will connect to tier j only if

$$j = \arg \max_{k \in \{1,2,3\}} P_k L_k(x), \quad (3.1)$$

where P_k is the transmission power of k^{th} tier, $L_k(x) = x_k^{-\alpha_k}$ is the path loss function where x is distance between typical user and serving BS and α_k is the path loss exponent.

The average received power at a user associated with MBS j ($j \in \phi_1$) is given as,

$$P_{r,1} = G_M \frac{P_1}{S} L_{j,M}(x), \quad (3.2)$$

where P_1 is MBS's transmit power, $L_{j,M}(x) = x^{-\alpha_1}$ is path loss function where α_1 is path loss exponent and G_M is the array gain given as $N - S + 1$ for zero forcing beamforming transmission [31]. It is evident from (3.2) that the array gain of massive MIMO macro cell tier has a prominent impact on user cell association. The average received power in case the user is associated with small cell tier i BS is,

$$P_{r,i} = P_i L_i(x), \quad \text{where } i = \{2, 3\}, \quad (3.3)$$

where P_i is small cell BS transmit power in the i^{th} tier and $L_i(x) = x_i^{-\alpha_i}$ is small cell path loss function with path loss exponent α_i .

3.2 Channel Model

We assume independent and identically distributed (i.i.d) Rayleigh fading channel for sub-6GHz links and independent Nakagami fading for mmWave links. The SINR of a typical user located at a distance x associated with the MBS is represented as

$$\text{SINR}_M^u = \frac{\frac{P_1}{S} h_{o,M} L_{o,M}(x)}{\sigma^2 + I_M + I_S}, \quad (3.4)$$

such that $I_M = \sum_{j \in \Phi_1 \setminus b_{o,M}} \frac{P_1}{S} h_{j,M} L_{j,M}(x_j)$ and $I_S = \sum_{q \in \Phi_2} P_q h_q L_q(x_q)$ are inter cell interference from the macro cell or small cell operating in sub-6GHz band except the serving BS $b_{o,M}$, while h_q is the small scale fading

gain from the interfering channel such that $h_q \sim \exp(1)$. Similarly, x_q is distance between the typical user and small cell BS q , while $h_{o,M}$ is the small scale fading gain of the typical user at the distance x from the serving BS such that $h_{o,M} \sim \Gamma(N - S + 1, 1)$ [31]. $h_{j,M}$ is small scale fading power gain such that $h_{j,M} \sim \Gamma(S, 1)$ [31], x_j is distance between typical user and MBS j , $L_q(x_q) = x_q^{-\alpha_2}$ and σ^2 is the noise power.

Similarly, the SINR of a typical user located at the distance x associated with the small cell operating at sub-6GHz band is represented as

$$\text{SINR}_S^u = \frac{P_2 h_{o,S} L_{o,S}(x)}{\sigma^2 + I_{\bar{M}} + I_{\bar{S}}}, \quad (3.5)$$

such that $I_{\bar{M}} = \sum_{j \in \Phi_1} \frac{P_j}{S} h_j L_j(x_j)$ and $I_{\bar{S}} = \sum_{q \in \Phi_2 \setminus b_{o,S}} P_2 h_{q,S} L_{q,S}(x_q)$. Here, $h_{q,S}$ is the small scale fading gain from the interfering channel such that $h_q \sim \exp(1)$ and x_q is the distance of the typical user from small cell BS q . Similarly, $h_{o,S}$ is the small scale fading gain of the typical user at the distance x from the serving BS such that $h_{o,S} \sim \exp(1)$ while h_j is small scale fading power gain such that $h_j \sim \Gamma(S, 1)$. Here, x_j is distance of the user from MBS j , $L_{q,S}(x_q) = x_q^{-\alpha_2}$ and $L_{o,S}(x) = x^{-\alpha_2}$ are path loss functions.

The SINR for the typical user associated with mmWave small cell is represented as

$$\text{SINR}_m = \frac{P_3 M_r M_t h_{o,m} L_{o,m}(x)}{\sigma^2 + P_3 \sum_{j \in L, N} \sum_{i \in \Phi_3 \setminus b_{o,m}} G_l h_{i,m} L_{i,m}(x_i)}, \quad (3.6)$$

where $L_{o,S}(x) = x^{-\alpha_3}$, $h_{o,m}$ is small scale fading gain where different Nakagami fading parameters are taken for LoS and NLoS links, M_r and M_t are the main lobe gains of the transmit and receive antennas, $j \in \{L, N\}$ identifies the interfering link as either LoS (L) or NLoS (N) and G_l is the directivity

gain of interfering BSs. It is assumed that both the BSs and the users are in perfect alignment with each other so the directivity gain of the desired link signal is given by $M_r M_t$. Beam direction is assumed to be independently and uniformly distributed between $(0, 2\pi]$. Hence G_l for $l = \{1, 2, 3, 4\}$ is given as,

$$G_l = \begin{cases} a_i = M_r M_t & \text{with prob. } p_i = \left(\frac{\theta_r}{2\pi} \frac{\theta_t}{2\pi}\right) \\ a_i = M_r m_t & \text{with prob. } p_i = \left(\frac{\theta_r}{2\pi} \left(1 - \frac{\theta_t}{2\pi}\right)\right) \\ a_i = m_r M_t & \text{with prob. } p_i = \left(\left(1 - \frac{\theta_r}{2\pi}\right) \frac{\theta_t}{2\pi}\right) \\ a_i = m_r m_t & \text{with prob. } p_i = \left(\left(1 - \frac{\theta_r}{2\pi}\right) \left(1 - \frac{\theta_t}{2\pi}\right)\right). \end{cases}$$

3.2.1 Blockage Model

A stochastic blockage model is assumed for mmWave small cells, where blockages are modeled as a rectangle Boolean scheme, based on random shape theory [29]. On the basis of this scheme, LoS probability function $p(R)$ is given by, $p(R) = e^{-\beta R}$ where R is the link distance and β is the dependent on statistics of blockages. The LoS probabilities for various links are assumed to be independent.

3.3 Performance Analysis

In this section, we perform stochastic modeling of user association probability for each tier based on probability density function (PDF) of distance between the typical user and serving BS and their coverage probability and rate is analyzed by extending existing analytical models to our network scenario.

3.3.1 Association Probability per Tier

Sub-6GHz Macro Cell tier

The association probability that a user is connected to MBS is given by,

$$A_1 = 2\pi\lambda_1 \int_0^\infty x \exp\left(-\pi\lambda_2 \left(\frac{P_2 S x^{\alpha_1}}{P_1(N-S+1)}\right)^{2/\alpha_2} - \pi\lambda_1 x^2 - 2\pi\lambda_3 \left(\frac{P_3 S}{P_1(N-S+1)}\right)^{2/\alpha_3} L(x)\right) dx, \quad (3.7)$$

where $L(x)$ is given by,

$$L(x) = \int_0^{\Delta_N(x)} t p(t) dt + \int_0^{\Delta_L(x)} t(1-p(t)) dt, \quad (3.8)$$

where $\Delta_N(x) = x^{\alpha_N/\alpha_L}$ and $\Delta_L(x) = x^{\alpha_L/\alpha_N}$. $L(x)$ is based on the independent thinning of ϕ_3 with LoS probability function $p(R)$, as described in section III. The probability density function of users distance to serving MBS, $f_{X_1}(x)$, is given as,

$$f_{X_1}(x) = \frac{2\pi\lambda_1}{A_1} x \exp\left(-\pi\lambda_2 \left(\frac{P_2 S x^{\alpha_1}}{P_1(N-S+1)}\right)^{2/\alpha_2} - \pi\lambda_1 x^2 - 2\pi\lambda_3 \left(\frac{P_3 S}{P_1(N-S+1)}\right)^{2/\alpha_3} L(x)\right). \quad (3.9)$$

Sub-6 GHz Small Cell tier

The association probability that a user is connected to sub-6GHz small cell BS is given by,

$$A_2 = 2\pi\lambda_2 \int_0^\infty x \exp\left(-\pi\lambda_2 x^2 - 2\pi\lambda_3 L(x) - \pi\lambda_1 \left(\frac{P_1(N-S+1)x^{\alpha_2}}{P_2 S}\right)^{2/\alpha_1}\right) dx, \quad (3.10)$$

where $L(x)$ is given by (3.8).

The probability density function of users distance to serving sub-6GHz small cell BS, $f_{X_2}(x)$, is given as,

$$f_{X_2}(x) = \frac{2\pi\lambda_2}{A_2} x \exp\left(-\pi\lambda_2 x^2 - 2\pi\lambda_3 L(x) - \pi\lambda_1 \left(\frac{P_1(N-S+1)x^{\alpha_2}}{P_2 S}\right)^{2/\alpha_1}\right). \quad (3.11)$$

mmWave Small Cell tier

The association probability that a user is connected to mmWave small cell BS is given as

$$A_3 = 1 - \sum_{k \in \{1,2\}} A_k. \quad (3.12)$$

The probability of associating with NLoS link is given by,

$$A_N = \Lambda_N \int_0^\infty \exp\left\{-2\pi\lambda_3 \int_0^{\Delta_N(x)} tp(t)dt\right\} f_N(x) dx x^{-\alpha_M} \quad (3.13)$$

Thus, the probability of associating with LoS link is $A_L = 1 - A_N$. Here, $f_N(x)$ is probability density function of the distance of the typical user to the NLoS BS given by, $f_N(x) = 2\pi\lambda_3 x(1-p(x))\exp(-2\pi\lambda_3 \int_0^x t(1-p(t))dt)/\Lambda_N$ and for LoS link, $f_L(x) = 2\pi\lambda_3 xp(x)\exp(-2\pi\lambda_3 \int_0^x tp(t)dt)/\Lambda_L$ [Eq. 4 of [22], [29], Theorem 8] where $\Lambda_N = 1 - \exp\{-2\pi\lambda_3 \int_0^\infty t(1-p(t))dt\}$ is probability of user having at least one NLoS link, likewise, $\Lambda_L = 1 - \exp\{-2\pi\lambda_3 \int_0^\infty tp(t)dt\}$ for LoS link.

PDF of the distance of user to serving BS given it is associated with LoS BS is $\hat{f}_L(x) = \frac{\Lambda_L f_L(x)}{A_L} \exp\left\{-2\pi\lambda_3 \int_0^{\Delta_L(x)} t(1-p(t))dt\right\}$ and for NLoS link $\hat{f}_N(x) = \frac{\Lambda_N f_N(x)}{A_N} \exp\left\{-2\pi\lambda_3 \int_0^{\Delta_N(x)} tp(t)dt\right\}$.

3.3.2 Coverage Probability

Coverage probability is the measure that the received SINR at a typical user is higher than a certain threshold, Mathematically

$$\begin{aligned}
 P_C^k(\Gamma) &= \Pr(\text{SINR}_k > \Gamma) \\
 &= \int_0^\infty \Pr(\text{SINR}_k > \Gamma | X_k = x) f_{X_k}(x) dx \\
 &= \int_0^\infty P^k(\Gamma, x) f_{X_k}(x) dx \quad \text{where } k = \{1, 2\}.
 \end{aligned} \tag{3.14}$$

The total SINR coverage probability, P_C , is calculated using law of total probability as

$$P_C = \sum_{r=1}^3 P_C^r A_r. \tag{3.15}$$

The coverage probability for a user associated with MBS is given by,

$$\begin{aligned}
 P^1(\Gamma, x) &= \sum_{l=0}^{N-S} \frac{(x^{\alpha_1})^l}{(l!)(-1)^l} \sum \frac{l!}{\prod_{j=1}^l n_j!(j!)^{n_j}} \\
 &\times \exp\left(-\frac{\Gamma \sigma^2 S x^{\alpha_1}}{P_1} - \Xi\left(\frac{\Gamma S x^{\alpha_1}}{P_1}\right)\right) \prod_{j=1}^l (\Psi^{(j)}(x^{\alpha_1}))^{n_j},
 \end{aligned} \tag{3.16}$$

where $\Xi(\cdot)$ and $\Psi^{(j)}(\cdot)$ is given as,

$$\begin{aligned}
 \Xi(q) &= 2\pi\lambda_1 \sum_{z=1}^S \binom{S}{z} \left(\frac{P_1}{S}\right)^z q^z \left(\frac{(-q\frac{P_1}{S})^{-z+\frac{2}{\alpha_1}}}{\alpha_1}\right) \\
 B_{(-q\frac{P_1}{S}x^{-\alpha_1})} &\left[z - \frac{2}{\alpha_1}, 1 - S\right] + 2\pi\lambda_2 q P_2 \frac{(J(x))^{\frac{2-\alpha_2}{\alpha_2}}}{\alpha_2 - 2} \\
 &{}_2F_1\left[\frac{\alpha_2 - 2}{\alpha_2}, 1; 2 - \frac{2}{\alpha_2}; -qP_2(J(x))^{-1}\right],
 \end{aligned} \tag{3.17}$$

$$\begin{aligned}
 \Psi^{(1)}(i) &= -\frac{\Gamma\sigma^2 Sx^{\alpha_1}}{P_1} - 2\pi\lambda_1 S\Gamma \frac{x^{2-\alpha_1}}{\alpha_1 - 2} \\
 {}_2F_1 \left[\frac{\alpha_1 - 2}{\alpha_1}, S + 1; 2 - \frac{2}{\alpha_1}; -i\Gamma x^{-\alpha_1} \right] &- 2\pi\lambda_2 \frac{\Gamma S}{P_1} \\
 \frac{(J(x))^{\frac{2-\alpha_2}{\alpha_2}}}{\alpha_2 - 2} {}_2F_1 \left[\frac{\alpha_2 - 2}{\alpha_2}, 2; 2 - \frac{2}{\alpha_2}; -\frac{i\Gamma S}{P_1} P_2(J(x))^{-1} \right], &
 \end{aligned} \tag{3.18}$$

$$\begin{aligned}
 \Psi^{(j)}(i) &= 2\pi\lambda_1 (-\Gamma)^{\frac{2}{\alpha_1}} \frac{(S + j - 1)!}{(S - 1)!} \frac{(i)^{-j + \frac{2}{\alpha_1}}}{\alpha_1} \\
 B_{(-\Gamma i x^{-\alpha_1})} \left[j - \frac{2}{\alpha_1}, 1 - S - j \right] &+ 2\pi\lambda_2 (j!) \frac{(i)^{-j + \frac{2}{\alpha_1}}}{\alpha_1} \\
 \left(-\frac{\Gamma S P_2}{P_1} \right)^{\frac{2}{\alpha_1}} B_{(-P_2 \frac{\Gamma S i}{P_1} (J(x))^{-\frac{\alpha_1}{\alpha_2}})} \left[j - \frac{2}{\alpha_1}, -j \right], &
 \end{aligned} \tag{3.19}$$

where $J(x) = \left(\frac{P_2 S x^{\alpha_1}}{(N-S+1)P_1} \right)$.

The coverage probability for a user associated with sub-6GHz small cell tier is given as,

$$\begin{aligned}
 P^2(\Gamma, x) &= \exp \left(-\frac{\Gamma\sigma^2 x^{\alpha_2}}{P_2} - 2\pi\lambda_1 \sum_{z=1}^S \binom{S}{z} \left(\frac{P_1 \Gamma x^{\alpha_2}}{S P_2} \right)^z \right. \\
 &\times \frac{\left(-\frac{\Gamma x^{\alpha_2} P_1}{S P_2} \right)^{-z + \frac{2}{\alpha_1}}}{\alpha_1} B_{\left(\frac{P_1 \Gamma x^{\alpha_2}}{S P_2} (H(x))^{-1} \right)} \left[z - \frac{2}{\alpha_1}, 1 - S \right] - \\
 &\left. 2\pi\lambda_2 \Gamma x^{\alpha_2} \frac{x^{2-\alpha_2}}{\alpha_2 - 2} \times {}_2F_1 \left[\frac{\alpha_2 - 2}{\alpha_2}, 1; 2 - \frac{2}{\alpha_2}; -\Gamma \right] \right), &
 \end{aligned} \tag{3.20}$$

where $H(x) = \left(\frac{N-S+1}{S P_2} P_1 x^{\alpha_2} \right)$. The proof can be found on similar lines as mentioned in [15] and is omitted here due to the space limitation.

The coverage probability for a user associated with mmWave small cell is given by,

$$P_C^3(\Gamma) = A_L P_{3,L}(\Gamma) + A_N P_{3,N}(\Gamma), \tag{3.21}$$

where $P_{3,L}$ and $P_{3,N}$, obtained by following [22], are given as,

$$P_{3,L} \approx \sum_{j=1}^{N_L} (-1)^{j+1} \binom{N_L}{j} \times \int_0^\infty \exp\left(\frac{-j\eta_L x^{\alpha_L} \Gamma \sigma^2}{M_r M_t} - C_j(\Gamma, x) - D_j(\Gamma, x)\right) \hat{f}_L(x) dx, \quad (3.22)$$

and

$$P_{3,N} \approx \sum_{j=1}^{N_N} (-1)^{j+1} \binom{N_N}{j} \times \int_0^\infty \exp\left(\frac{-j\eta_N x^{\alpha_N} \Gamma \sigma^2}{M_r M_t} - E_j(\Gamma, x) - V_j(\Gamma, x)\right) \hat{f}_N(x) dx. \quad (3.23)$$

where

$$C_j(\Gamma, x) = 2\pi\lambda_3 \sum_{i=1}^4 p_i \int_x^\infty F\left(N_L, \frac{j\eta_L \hat{a}_i \Gamma x^{\alpha_L}}{N_L t^{\alpha_L}}\right) p(t) dt, \quad (3.24)$$

$$D_j(\Gamma, x) = 2\pi\lambda_3 \sum_{i=1}^4 p_i \int_{\Delta_L(x)}^\infty F\left(N_N, \frac{j\eta_L \hat{a}_i \Gamma x^{\alpha_L}}{N_N t^{\alpha_N}}\right) (1-p(t)) dt, \quad (3.25)$$

$$E_j(\Gamma, x) = 2\pi\lambda_3 \sum_{i=1}^4 p_i \int_{\Delta_N(x)}^\infty F\left(N_L, \frac{j\eta_N \hat{a}_i \Gamma x^{\alpha_N}}{N_L t^{\alpha_L}}\right) p(t) dt, \quad (3.26)$$

$$V_j(\Gamma, x) = 2\pi\lambda_3 \sum_{i=1}^4 p_i \int_x^\infty F\left(N_N, \frac{j\eta_N \hat{a}_i \Gamma x^{\alpha_N}}{N_N t^{\alpha_N}}\right) (1-p(t)) dt, \quad (3.27)$$

and $F(N, x) = 1 - 1/(1+x)^N$. Here $\eta_L = N_L(N_L!)^{-\frac{1}{N_L}}$ and $\eta_N = N_N(N_N!)^{-\frac{1}{N_N}}$.

Parameter $\hat{a}_i = a_i/M_r M_t$, a_i and p_i are defined in Section III.

3.3.3 Rate Coverage Probability

We define the instantaneous downlink coverage rate for typical user similar to SINR coverage probability, such that the rate is higher than a certain threshold $\rho > 0$ for an associated tier k defined as

$$\begin{aligned} R_C^k &= \Pr(\text{Rate}_k > \rho) = \Pr(W \log(1 + \text{SINR}_k) > \rho) \\ &= \Pr(\text{SINR}_k > 2^{\frac{\rho}{W}} - 1) = P_C^k(2^{\frac{\rho}{W}} - 1), \end{aligned} \quad (3.28)$$

where W is the total available bandwidth at the BS.

3.4 Simulation and Numerical Results

In this section, we evaluate the numerical results for coverage and rate to study the influence of massive MIMO enabled macro tier on HetNet performance. A 3-tier HetNet is taken with MBS density $\lambda_1 = (250000 \times \pi)^{-1}$, λ_2 and λ_3 are taken multiples of MBS density. The sub-6GHz tiers are assumed to be operating at 1GHz carrier frequency, $W = 10\text{MHz}$ bandwidth, path loss exponents $\alpha_1 = 3.5$, $\alpha_2 = 4$ and transmit power $P_1 = 46\text{dBm}$ and $P_2 = 30\text{dBm}$, respectively. Likewise for mmWave tier, the operating frequency is 28GHz, has 100MHz bandwidth, path loss exponent for LoS $\alpha_L = 2$ and for NLoS $\alpha_N = 4$ and transmit power $P_3 = 30\text{dBm}$. Nakagami

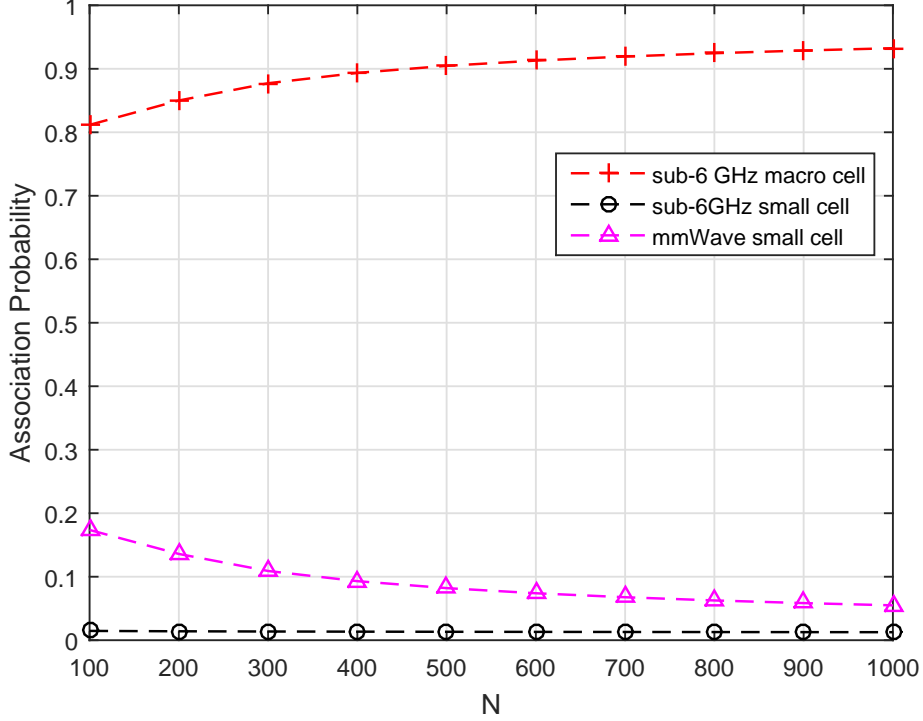


Figure 3.2: Association probability versus N with $\lambda_2 = \lambda_3 = 30\lambda_1$ and $S = 5$

fading parameters for mmWave tier, N_N and N_L , are assumed to be positive integers, 2 and 3, respectively. Array gains for all angles in main lobe are taken $M_r = 10\text{dB}$ and $M_t = 10\text{dB}$ and for the side lobes $m_r = -10\text{dB}$ and $m_t = 0\text{dB}$ gains are fixed. Main lobe beamwidth is taken to be $\theta_r = 90^\circ$ and $\theta_t = 30^\circ$. Noise $\sigma^2 = -90\text{dBm}$ is taken with noise figure of 10dB. For the LoS probability function $p(R) = e^{(-\beta R)}$, β is takes as $1/\beta = 141.4$ meters.

In Fig. 3.2 we observe the effect of increasing the number of antennas N on association probability of each tier. It is observed that association with macro BSs is directly proportional to the number of antennas on each BS and it prominently effects the user association with other tiers. This can be attributed to the higher array gains because of higher antenna density at

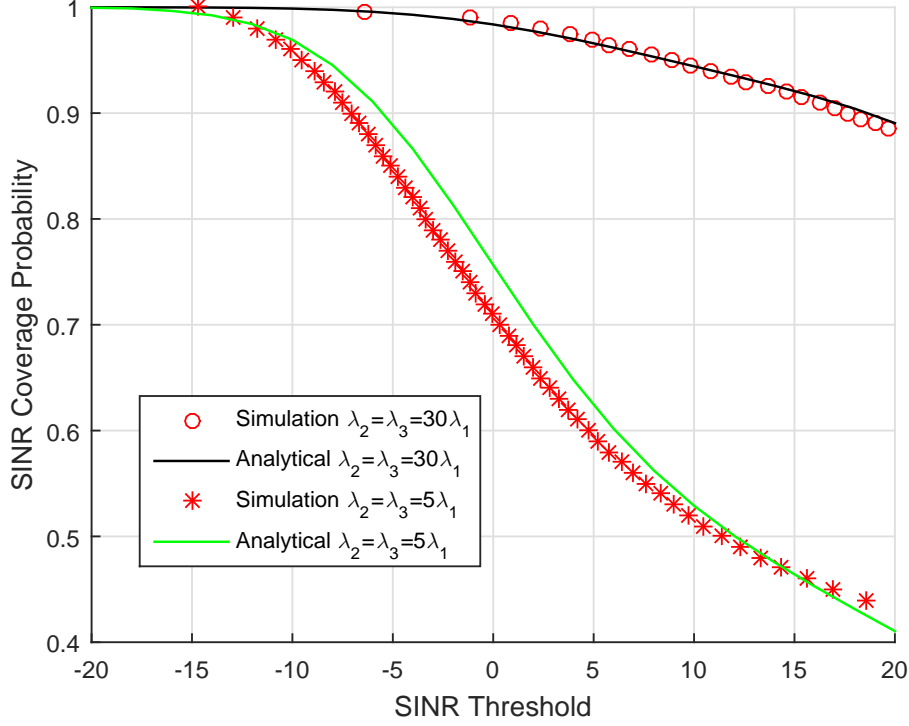


Figure 3.3: SINR coverage probability $P_C(\Gamma)$ versus SINR threshold Γ for $N = 4$ and $S = 2$

macro BSs. Other reason is that macro BSs have greater transmit power than small cell BSs. After macro BSs most of the load is managed by mmWave BSs due to their favourable SINR distribution and larger available bandwidth compared to the sub-6GHz small cell BSs.

Fig. 3.3 shows the network coverage probability P_C for different small cell BS densities. The graph shows that as small cell BS density increases, more users are offloaded to small cells and it significantly improves the SINR coverage of the network. Since small cells operate at lower power this may lead to power efficient network where high power macro BS have lower traffic but it comes at the cost of high small cell BS deployment. The macro cells may serve to provide better coverage at cell edges but within them small

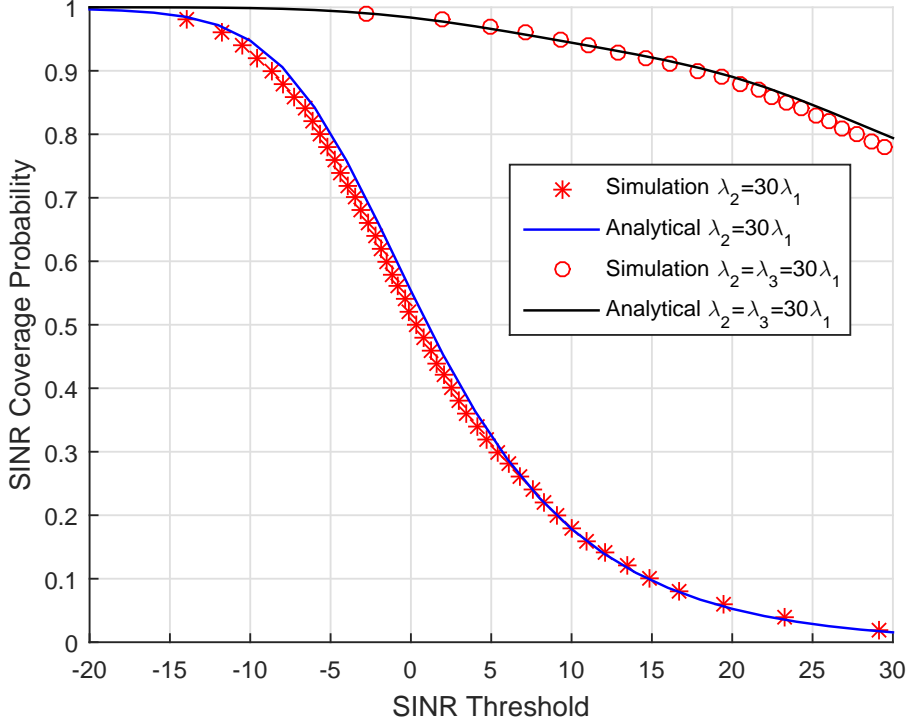


Figure 3.4: SINR coverage probability $P_C(\Gamma)$ versus SINR threshold Γ for $N = 4$ and $S = 2$

cells provide better coverage. Moreover, it can be observed that simulation results and analytical results are tightly bound to each other that validates the model.

Fig. 3.4 shows the network coverage probability comparison of 2-tier network with sub-6GHz macro and small cells and 3-tier network with mmWave small cells. The graph shows that the mmWave tier has significant contribution to SINR coverage probability. This can be attributed to the favourable SINR distribution, larger available bandwidth and higher density of mmWave cells. Macro cells may serve to provide better coverage at cell edges but within them small cells provide better coverage. Moreover, it can be observed that simulation results and analytical results are tightly bound to each other that

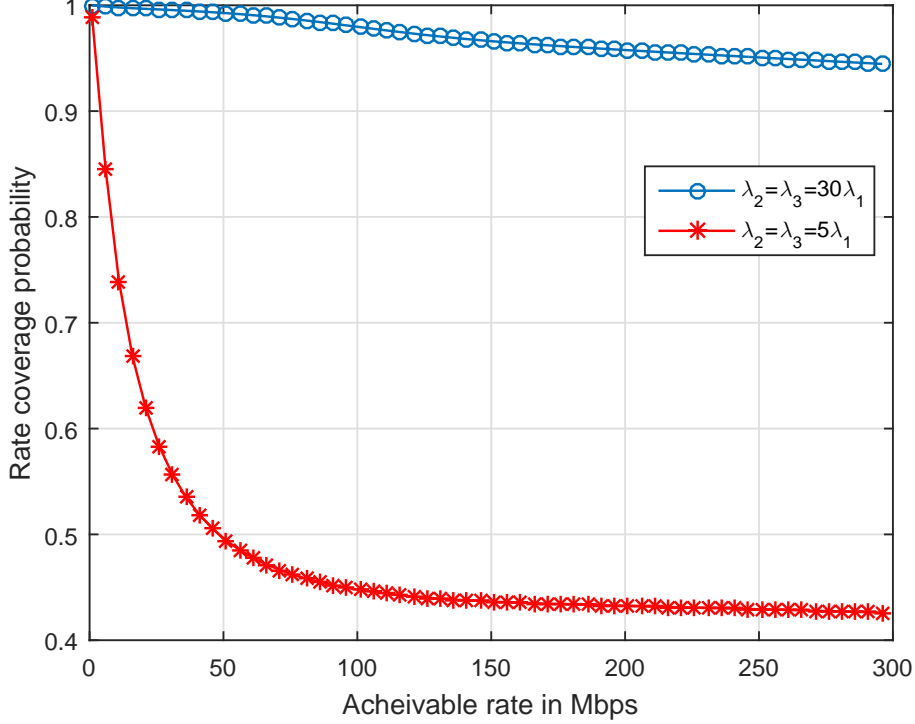


Figure 3.5: Rate coverage probability R_C verses rate threshold ρ for $N = 4$ and $S = 2$

validates the model.

Fig. 3.5 shows the rate coverage probability verses rate threshold for different small cells BS density. The graph shows that as the small cell BS density increases, rate increases drastically. This is due to the fact that small cell BSs form better links to the users when their deployment density is high and users associated with mmWave small cells have greater allocated bandwidth.

In Fig. 3.6 we compare the achievable rates for each network tier to see their contribution towards total network rate R_C . It is observed that the mmwave tier which has significantly small cell size compared to conventional sub-6GHz macro cells outperforms both sub-6GHz tiers though sub-6GHz

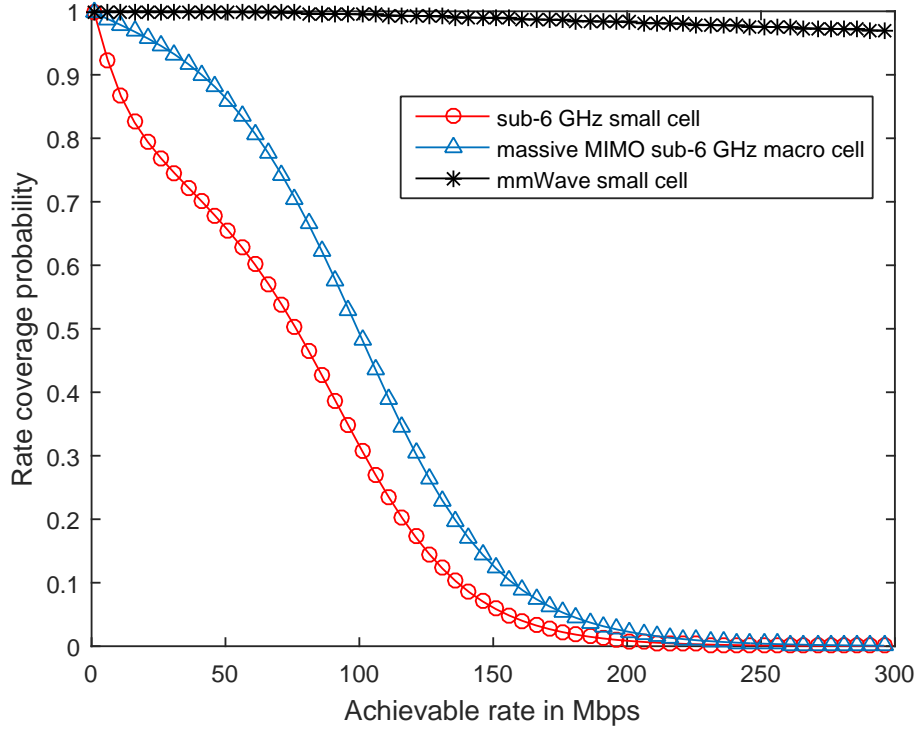


Figure 3.6: Rate coverage probability R_C^k versus rate threshold ρ for $\lambda_2 = \lambda_3 = 30\lambda_1$, $N = 4$ and $S = 2$

and mmWave small cells have same BS density. This is due to mmWave cells high bandwidth and favourable SINR distribution. After mmWave tier, macro cell has better rate coverage because of high transmit power.

Chapter 4

5G Green Hybrid HetNets

Secrecy Analysis

In this chapter, we use stochastic geometry for the analysis of a 3-tier network composed of mmWave and sub 6-GHz small cells overlaid massive MIMO-enabled sub 6-GHz macro cells. We analyze the network performance in terms of reliable and secure downlink transmission. To the best of our knowledge, no prior work has analyzed secrecy and connection outage of mmWave small cells coexisting with traditional HetNets with massive MIMO enabled macro BSs (MBSs) in the presence of eavesdropper. The mmWave and sub-6GHz small cells BSs are deployed at higher density than MBSs and user association, connection outage, secrecy outage, area spectral efficiency (ASE) and energy efficiency (EE) trends are discussed.

4.1 System Model

We consider the time-division duplex (TDD) secure downlink transmission scenario of a three-tier HetNet comprising of sub-6GHz macro cells overlaid with small cells operating at sub-6GHz and mmWave frequency band. It is assumed that sub-6GHz macro cell base stations (MBSs) are provided with large antenna arrays. The sub-6GHz small cells constitute tier 2 while tier 3 constitutes small cells operating at mmWave frequency band. The BSs of each k^{th} tier are uniformly located following a two dimensional homogeneous Poisson point process (HPPP) Φ_k with density λ_k where $k = \{1, 2, 3\}$. The user equipment and eavesdroppers are also uniformly distributed as HPPP Φ_u and Φ_e with density λ_u and λ_e , respectively. Massive MIMO is implemented at the macro cells where each MBS has N antennas which simultaneously transmit to S users where $N \gg S \geq 1$ [36]. All the small cell BSs and users are single antenna nodes. Zero forcing beamforming (ZFBF) is adopted by each MBS for transmitting S data streams with equal power assignment. It is considered that the downlink channel state information (CSI) is known at the MBS [15]. The performance of the network is analyzed for a typical user located at the origin, in accordance with Slivnyak's Theorem. The mmWave small cells can form either line-of-sight (LoS) or non-line-of-sight (NLoS) link to the typical user. Thus, we divide Φ_3 , by applying independent thinning theorem, to Φ_3^L and Φ_3^N as PPPs of LoS and NLoS mmWave small cells, respectively, using LoS probability function $p(R)$, to determine if a link of length R is LoS or NLoS [22]. Therefore, Φ_3^L and Φ_3^N have the densities $p(R)\lambda_3$ and $(1 - p(R))\lambda_3$, respectively. The LoS probability function $p(R)$ is discussed in detail in Section II-C.

4.1.1 Downlink User Association

An open access scheme has been assumed such that user has the flexibility to connect to any tier BS based on maximum average received power, i.e., a user will connect to tier j only if

$$j = \arg \max_{k \in \{1,2,3\}} P_k L_k(x), \quad (4.1)$$

where P_k is the transmission power of the k^{th} tier, $L_k(x) = x_k^{-\alpha_k}$ is the path loss function where x is distance between typical user and serving BS and α_k is the path loss exponent.

The average received power at a user which is connected with the MBS ($j \in \phi_1$) is given as,

$$P_{r,1} = G_M \frac{P_1}{S} L_{j,M}(x), \quad (4.2)$$

where G_M is the array gain, P_1 is the transmit power of MBS, $L_{j,M}(x) = x^{-\alpha_1}$ is path loss function where α_1 is path loss exponent of the macro tier. The array gain G_M is given as $N - S + 1$ for ZFBF transmission [31]. The average received power at the user connected with small cell tier BS is given as

$$P_{r,i} = P_i L_i(x), \quad \text{where } i = \{2, 3\}, \quad (4.3)$$

where P_i is small cell BS transmit power in the i^{th} tier and $L_i(x) = x_i^{-\alpha_i}$ is small cell path loss function with path loss exponent α_i .

4.1.2 Channel Model

We consider independent and identically distributed (i.i.d) Rayleigh fading channel for sub-6GHz links and independent Nakagami fading for mmWave

links. The received signal-to-interference-plus-noise ratio (SINR) for a typical user and any eavesdropper associated with the MBS $b_{o,M}$ is represented as

$$\text{SINR}_M^u = \frac{\frac{P_1}{S} h_{o,M} L_{o,M}(x)}{\sigma^2 + \sum_{j \in \Phi_1 \setminus b_{o,M}} \frac{P_1}{S} h_{j,M} L_{j,M}(x_j) + I_S}, \quad (4.4)$$

$$\text{SINR}_M^e = \frac{\frac{P_1}{S} h_{e,M} r_e^{-\alpha_1}}{\sigma^2 + \sum_{j \in \Phi_1} \frac{P_1}{S} h_{j,M} L_{j,M}(x_j) + I_S}, \quad (4.5)$$

where $I_S = \sum_{q \in \Phi_2} P_q h_q L_q(x_q)$ is the inter cell interference from the small cell operating in sub-6GHz band, h_q is the small scale fading gain from the interfering channel such that $h_q \sim \exp(1)$. Similarly, x_q is the distance between the typical user and small cell BS q , while $h_{o,M}$ and $h_{e,M}$ are the small scale fading gains of the typical user at the distance x and eavesdropper at the distance r_e from the serving BS such that $h_{o,M} \sim \Gamma(N - S + 1, 1)$ [31]. In (4.5), $h_{j,M}$ is small scale fading power gain such that $h_{j,M} \sim \Gamma(S, 1)$, x_j is distance between typical user and MBS j , $L_q(x_q) = x_q^{-\alpha_2}$ and σ^2 is the noise power.

The SINR of a typical user located at a distance x and any eavesdropper at distance r_e associated with the small cell BS $b_{o,S}$ operating at sub-6GHz band is represented as

$$\text{SINR}_S^u = \frac{P_2 h_{o,S} L_{o,S}(x)}{\sigma^2 + \sum_{q \in \Phi_2 \setminus b_{o,S}} P_2 h_{q,S} L_{q,S}(x_q) + I_{\bar{M}}}, \quad (4.6)$$

$$\text{SINR}_S^e = \frac{P_2 h_{e,S} r_e^{-\alpha_2}}{\sigma^2 + \sum_{q \in \Phi_2} P_2 h_{q,S} L_{q,S}(x_q) + I_{\bar{M}}}, \quad (4.7)$$

where $I_{\bar{M}} = \sum_{j \in \Phi_1} \frac{P_j}{S} h_j L_j(x_j)$ is the intercell interference from macro cells, $L_{q,S}(x_q) = x_q^{-\alpha_2}$ and $L_{o,S}(x) = x^{-\alpha_2}$. Here, $h_{q,S}$ is the small scale fading gain from the interfering channel such that $h_q \sim \exp(1)$ and x_q is the distance

of the typical user from small cell BS q . Similarly, $h_{o,S}$ and $h_{e,S}$ are the small scale fading gain of the typical user such that $h_{o,S} \sim \exp(1)$ while h_j is small scale fading power gain such that $h_j \sim \Gamma(S, 1)$. Here, x_j is distance of the user from MBS j , $L_{q,S}(x_q) = x_q^{-\alpha_2}$ and $L_{o,S}(x) = x^{-\alpha_2}$ are path loss functions.

The SINR for the typical user and any eavesdropper associated with mmWave small cell $b_{o,m}$ is represented as

$$\text{SINR}_m^u = \frac{P_3 M_r M_t h_{o,m} L_{o,m}(x)}{\sigma^2 + P_3 \sum_{j \in \{L, N\}} \sum_{i \in \Phi_3^j \setminus b_{o,m}} G_l h_{i,m} L_{i,m}(x_i)}, \quad (4.8)$$

$$\text{SINR}_m^e = \frac{P_3 G_e h_{e,m} r_e^{-\alpha_3^{(j)}}}{\sigma^2 + P_3 \sum_{j \in \{L, N\}} \sum_{i \in \Phi_3^j} G_l h_{i,m} L_{i,m}(x_i)}, \quad (4.9)$$

where $L_{o,m}(x) = x^{-\alpha_3^{(j)}}$, $h_{o,m}$ and $h_{e,m}$ are small scale fading gain where Nakagami fading parameter for LoS and NLoS links are unique positive integers N_j , M_r and M_t are the main lobe gains of the transmit and receive antennas, G_l and G_e are the directivity gains of interfering BSs and eavesdropper and $j \in \{L, N\}$ identifies the interfering link as either LoS (L) or NLoS (N). We assume that both the BSs and the users have their main lobe aligned in the direction of dominant propagation path so the directivity gain of the desired link signal is given by $M_r M_t$. Beam direction is assumed to be independently and uniformly distributed between $(0, 2\pi]$. Hence G_l for

$l = \{1, 2, 3, 4\}$ is given as,

$$G_l = \begin{cases} a_l = M_r M_t & \text{with prob. } p_l = \left(\frac{\theta_r}{2\pi} \frac{\theta_t}{2\pi}\right) \\ a_l = M_r m_t & \text{with prob. } p_l = \left(\frac{\theta_r}{2\pi} \left(1 - \frac{\theta_t}{2\pi}\right)\right) \\ a_l = m_r M_t & \text{with prob. } p_l = \left(\left(1 - \frac{\theta_r}{2\pi}\right) \frac{\theta_t}{2\pi}\right) \\ a_l = m_r m_t & \text{with prob. } p_l = \left(\left(1 - \frac{\theta_r}{2\pi}\right) \left(1 - \frac{\theta_t}{2\pi}\right)\right). \end{cases}$$

4.1.3 Blockage Model

A blockage model based on stochastic geometry approach is assumed for mmWave small cells. Based on random shape theory, blockages are modeled as a rectangle Boolean scheme [29]. Hence the LoS probability function $p(R)$ is given as, $p(R) = e^{-\beta R}$ where β is the dependent on statistics of blockages and R is the BS to typical user link distance. The LoS probabilities for various links are considered independent of each other.

4.1.4 Area Spectral Efficiency and Energy Efficiency

We define ASE of the system as the total rate in a unit area normalized by the bandwidth, given as

$$\eta_{ASE} = \sum_{k=1}^3 \lambda_k \log_2(1 + \Gamma) P_C^k(\Gamma), \quad (4.10)$$

where $P_C^k(\Gamma)$ is coverage probability conditioned on the user associated with tier k and Γ is SINR threshold.

The EE of the system is defined as

$$\eta_{EE} = \frac{\lambda_u \sum_{k=1}^3 A_k W_k \log_2(1 + \Gamma) P_C^k(\Gamma)}{\sum_{k=1}^3 \lambda_k \left(\frac{1}{\epsilon} P_k + \rho_c\right)}, \quad (4.11)$$

where W_k is the bandwidth allocated to user connected to the BS in tier k , ϵ is the amplifier efficiency, ρ_c is the load independent circuit power and λ_u is user density.

4.2 Performance Analysis

In this section, we perform stochastic modeling of typical user association probability for each tier followed by connection and secrecy outage probability of proposed network scenario.

4.2.1 Reliable and Secure Transmission Characterization

In the proposed network scenario, it is assumed that all tier links are eavesdropped and for enhanced secrecy, a secrecy coding scheme called Wyner code is adopted at each link [?]. Based on this scheme, we need to specify two kind of rates at the transmitter, i.e., rate of the transmitted message signal R_m , and rate of transmitted code words R_c . In the considered network scenario, when a BS of any tier intends to make a reliable and secure transmission, depending of the choice of R_m and R_c at the BS, the following outage events are bound to occur.

a. Connection outage occurs when the capacity of the link between typical user and its associated BS falls below the transmitted message rate R_m , i.e., SINR of the received signal is below a certain threshold. Hence, we define connection outage probability as $P_{co}^k(\Gamma) = \Pr(\text{SINR}_k^u < \Gamma)$.

b. Secrecy outage occurs when the capacity of the channel between the serving BS and any eavesdropper is above the rate R_e and message security is

breached, i.e., received SINR at any eavesdropper is above a certain threshold. Hence, we define secrecy outage probability as $P_{so}^k(\Gamma_e) = \Pr(\text{SINR}_k^e > \Gamma_e)$.

4.2.2 Association Probability

Sub-6GHz Macro Cell tier

The association probability that a typical user is connected to the MBS is given by,

$$A_1 = 2\pi\lambda_1 \int_0^\infty x \exp\left(-\pi\lambda_2 \left(\frac{P_2 S x^{\alpha_1}}{P_1(N-S+1)}\right)^{2/\alpha_2} - \pi\lambda_1 x^2 - 2\pi\lambda_3 \left(\frac{P_3 S}{P_1(N-S+1)}\right)^{2/\alpha_3} L(x)\right) dx, \quad (4.12)$$

where $L(x)$ is given by,

$$L(x) = \int_0^{\Delta_N(x)} t p(t) dt + \int_0^{\Delta_L(x)} t(1-p(t)) dt, \quad (4.13)$$

where $\Delta_N(x) = x^{\alpha_N/\alpha_L}$ and $\Delta_L(x) = x^{\alpha_L/\alpha_N}$ that follows from the independent thinning of ϕ_3 with LoS probability function $p(R)$ as discussed in Section II. The probability density function (PDF) of users distance to serving MBS, $f_{X_1}(x)$, is given as,

$$f_{X_1}(x) = \frac{2\pi\lambda_1}{A_1} x \exp\left(-\pi\lambda_2 \left(\frac{P_2 S x^{\alpha_1}}{P_1(N-S+1)}\right)^{2/\alpha_2} - \pi\lambda_1 x^2 - 2\pi\lambda_3 \left(\frac{P_3 S}{P_1(N-S+1)}\right)^{2/\alpha_3} L(x)\right). \quad (4.14)$$

Sub-6 GHz Small Cell tier

The association probability that a typical user is connected to sub-6GHz small cell BS is given by,

$$A_2 = 2\pi\lambda_2 \int_0^\infty x \exp\left(-\pi\lambda_2 x^2 - 2\pi\lambda_3 L(x) - \pi\lambda_1 \left(\frac{P_1(N-S+1)x^{\alpha_2}}{P_2 S}\right)^{2/\alpha_1}\right) dx. \quad (4.15)$$

The PDF of the distance of the typical user to serving sub-6GHz small cell BS, $f_{X_2}(x)$, is given as,

$$f_{X_2}(x) = \frac{2\pi\lambda_2}{A_2} x \exp\left(-\pi\lambda_2 x^2 - 2\pi\lambda_3 L(x) - \pi\lambda_1 \left(\frac{P_1(N-S+1)x^{\alpha_2}}{P_2 S}\right)^{2/\alpha_1}\right). \quad (4.16)$$

mmWave Small Cell tier

The association probability that a user is associated to a mmWave small cell BS is given as

$$A_3 = 1 - \sum_{k \in \{1,2\}} A_k. \quad (4.17)$$

For mmWave links, the probability of connecting with NLoS link is given by, $A_N = \Lambda_N \int_0^\infty \exp\left\{-2\pi\lambda_3 \int_0^{\Delta_N(x)} tp(t)dt\right\} f_N(x) dx$ [22]. Hence, the probability of connecting with LoS link is $A_L = 1 - A_N$.

Here, $f_N(x) = 2\pi\lambda_3 x(1-p(x))\exp(-2\pi\lambda_3 \int_0^x t(1-p(t))dt)/\Lambda_N$ is the PDF of the distance of the typical user to the NLoS BS and for LoS link, $f_L(x) = 2\pi\lambda_3 xp(x)\exp(-2\pi\lambda_3 \int_0^x tp(t)dt)/\Lambda_L$ [Eq. 4 of [22], [29], Theorem 8] where $\Lambda_N = 1 - \exp\left\{-2\pi\lambda_3 \int_0^\infty t(1-p(t))dt\right\}$ is probability that the user has at least one NLoS link, likewise, $\Lambda_L = 1 - \exp\left\{-2\pi\lambda_3 \int_0^\infty tp(t)dt\right\}$ for

LoS link.

The PDF of the distance of the typical user to serving BS given that it is connected with LoS link is $\hat{f}_L(x) = \frac{\Lambda_L f_L(x)}{A_L} \exp \left\{ -2\pi\lambda_3 \int_0^{\Delta_L(x)} t(1-p(t))dt \right\}$ and for NLoS link $\hat{f}_N(x) = \frac{\Lambda_N f_N(x)}{A_N} \exp \left\{ -2\pi\lambda_3 \int_0^{\Delta_N(x)} tp(t)dt \right\}$.

4.2.3 Connection Outage Probability

Connection outage probability of a typical user associated with sub-6GHz macro or small cell BS is given as

$$\begin{aligned} P_{co}^k(\Gamma) &= \Pr(\text{SINR}_k^u < \Gamma) = 1 - \Pr(\text{SINR}_k^u > \Gamma) \\ &= 1 - \int_0^\infty \Pr(\text{SINR}_k^u > \Gamma | X_k = x) f_{X_k}(x) dx \\ &= 1 - \int_0^\infty P^k(\Gamma, x) f_{X_k}(x) dx \quad \text{where } k = \{1, 2\}. \end{aligned}$$

Here $P^1(\Gamma, x)$ for a typical user associated with MBS at the distance x is given by

$$\begin{aligned} P^1(\Gamma, x) &= \sum_{l=0}^{N-S} \frac{(x^{\alpha_1})^l}{(l!)(-1)^l} \sum \frac{l!}{\prod_{j=1}^l n_j!(j!)^{n_j}} \\ &\times \exp\left(-\frac{\Gamma\sigma^2 S x^{\alpha_1}}{P_1} - \Xi\left(\frac{\Gamma S x^{\alpha_1}}{P_1}\right)\right) \prod_{j=1}^l (\Psi^{(j)}(x^{\alpha_1}))^{n_j}, \end{aligned} \quad (4.18)$$

where $\Xi(\cdot)$ and $\Psi^{(j)}(\cdot)$ are given as,

$$\begin{aligned} \Xi(q) &= 2\pi\lambda_1 \sum_{z=1}^S \binom{S}{z} \left(\frac{P_1}{S}\right)^z q^z \left(\frac{(-q\frac{P_1}{S})^{-z+\frac{2}{\alpha_1}}}{\alpha_1}\right) \\ &B_{(-q\frac{P_1}{S}x^{-\alpha_1})} \left[z - \frac{2}{\alpha_1}, 1 - S \right] + 2\pi\lambda_2 q P_2 \frac{(J(x))^{\frac{2-\alpha_2}{\alpha_2}}}{\alpha_2 - 2} \\ &{}_2F_1 \left[\frac{\alpha_2 - 2}{\alpha_2}, 1; 2 - \frac{2}{\alpha_2}; -qP_2(J(x))^{-1} \right], \end{aligned} \quad (4.19)$$

$$\begin{aligned} \Psi^{(1)}(i) &= -\frac{\Gamma\sigma^2 S x^{\alpha_1}}{P_1} - 2\pi\lambda_1 S \Gamma \frac{x^{2-\alpha_1}}{\alpha_1 - 2} \\ &{}_2F_1 \left[\frac{\alpha_1 - 2}{\alpha_1}, S + 1; 2 - \frac{2}{\alpha_1}; -i\Gamma x^{-\alpha_1} \right] - 2\pi\lambda_2 \frac{\Gamma S}{P_1} \\ &\frac{(J(x))^{\frac{2-\alpha_2}{\alpha_2}}}{\alpha_2 - 2} {}_2F_1 \left[\frac{\alpha_2 - 2}{\alpha_2}, 2; 2 - \frac{2}{\alpha_2}; -\frac{i\Gamma S}{P_1} P_2 (J(x))^{-1} \right], \end{aligned} \quad (4.20)$$

$$\begin{aligned} \Psi^{(j)}(i) &= 2\pi\lambda_1 (-\Gamma)^{\frac{2}{\alpha_1}} \frac{(S + j - 1)! (i)^{-j+\frac{2}{\alpha_1}}}{(S - 1)! \alpha_1} \\ &B_{(-\Gamma i x^{-\alpha_1})} \left[j - \frac{2}{\alpha_1}, 1 - S - j \right] + 2\pi\lambda_2 (j!) \frac{(i)^{-j+\frac{2}{\alpha_1}}}{\alpha_1} \\ &\left(-\frac{\Gamma S P_2}{P_1} \right)^{\frac{2}{\alpha_1}} B_{(-P_2 \frac{\Gamma S i}{P_1} (J(x))^{\frac{-\alpha_1}{\alpha_2}})} \left[j - \frac{2}{\alpha_1}, -j \right], \end{aligned} \quad (4.21)$$

where $J(x) = \left(\frac{P_2 S x^{\alpha_1}}{(N-S+1)P_1} \right)$.

Similarly, $P^2(\Gamma, x)$ for a typical user associated with sub-6GHz small cell BS at distance x is given as,

$$\begin{aligned} P^2(\Gamma, x) &= \exp \left(-\frac{\Gamma\sigma^2 x^{\alpha_2}}{P_2} - 2\pi\lambda_1 \sum_{z=1}^S \binom{S}{z} \left(\frac{P_1 \Gamma x^{\alpha_2}}{S P_2}\right)^z \right. \\ &\times \frac{(-\frac{\Gamma x^{\alpha_2} P_1}{S P_2})^{-z+\frac{2}{\alpha_1}}}{\alpha_1} B_{(\frac{P_1 \Gamma x^{\alpha_2}}{S P_2} (H(x))^{-1})} \left[z - \frac{2}{\alpha_1}, 1 - S \right] - \\ &\left. 2\pi\lambda_2 \Gamma x^{\alpha_2} \frac{x^{2-\alpha_2}}{\alpha_2 - 2} \times {}_2F_1 \left[\frac{\alpha_2 - 2}{\alpha_2}, 1; 2 - \frac{2}{\alpha_2}; -\Gamma \right] \right), \end{aligned} \quad (4.22)$$

where $H(x) = \left(\frac{N-S+1}{SP_2} P_1 x^{\alpha_2}\right)$. The proof can be found on similar lines as mentioned in [15].

The connection outage probability for a user associated with mmWave small cell is given by,

$$P_{co}^3(\Gamma) = 1 - \left[A_L P_{3,L}(\Gamma) + A_N P_{3,N}(\Gamma) \right], \quad (4.23)$$

where $P_{3,L}$ and $P_{3,N}$ are given as,

$$P_{3,L} \approx \sum_{j=1}^{N_L} (-1)^{j+1} \binom{N_L}{j} \times \int_0^\infty \exp\left(\frac{-j\eta_L x^{\alpha_L} \Gamma \sigma^2}{M_r M_t} - C_j(\Gamma, x) - D_j(\Gamma, x)\right) \hat{f}_L(x) dx,$$

and

$$P_{3,N} \approx \sum_{j=1}^{N_N} (-1)^{j+1} \binom{N_N}{j} \times \int_0^\infty \exp\left(\frac{-j\eta_N x^{\alpha_N} \Gamma \sigma^2}{M_r M_t} - E_j(\Gamma, x) - V_j(\Gamma, x)\right) \hat{f}_N(x) dx.$$

where

$$C_j(\Gamma, x) = 2\pi\lambda_3 \sum_{i=1}^4 p_i \int_x^\infty F\left(N_L, \frac{j\eta_L \hat{a}_i \Gamma x^{\alpha_L}}{N_L t^{\alpha_L}}\right) p(t) t dt,$$

$$D_j(\Gamma, x) = 2\pi\lambda_3 \sum_{i=1}^4 p_i \int_{\Delta_L(x)}^\infty F\left(N_N, \frac{j\eta_L \hat{a}_i \Gamma x^{\alpha_L}}{N_N t^{\alpha_N}}\right) (1-p(t)) t dt,$$

$$E_j(\Gamma, x) = 2\pi\lambda_3 \sum_{i=1}^4 p_i \int_{\Delta_N(x)}^\infty F\left(N_L, \frac{j\eta_N \hat{a}_i \Gamma x^{\alpha_N}}{N_L t^{\alpha_L}}\right) p(t) t dt,$$

$$V_j(\Gamma, x) = 2\pi\lambda_3 \sum_{i=1}^4 p_i \int_x^\infty F\left(N_N, \frac{j\eta_N \hat{a}_i \Gamma x^{\alpha_N}}{N_N t^{\alpha_N}}\right) (1-p(t)) t dt,$$

and $F(N, x) = 1 - 1/(1+x)^N$. Here $\eta_L = N_L(N_L!)^{-\frac{1}{N_L}}$ and $\eta_N = N_N(N_N!)^{-\frac{1}{N_N}}$.

Parameter $\hat{a}_i = a_i/M_r M_t$, a_i and p_i are defined in Section II. The proof can be found on similar lines as mentioned in [22] and is omitted here due to the space limitation.

The total connection outage probability, P_{co} , is calculated using law of total probability as

$$P_{co} = \sum_{k=1}^3 P_{co}^k A_k. \quad (4.24)$$

4.2.4 Secrecy Outage Probability

The secrecy outage probability is the measure that at least one of the eavesdroppers is causing the secrecy breach. It is defined for a typical link of k^{th} tier as

$$\begin{aligned} P_{so}^k(\Gamma_e) &= \Pr(\text{SINR}_k^e < \Gamma_e) = 1 - \Pr(\text{SINR}_k^e > \Gamma_e) \\ &\stackrel{(a)}{=} 1 - \mathbb{E}_{\phi_k} \left[\mathbb{E}_{\phi_e} \left[\prod_{e \in \phi_e} \left(1 - \Pr(\text{SINR}_k^e > \Gamma_e) \right) \right] \right] \\ &\stackrel{(b)}{=} 1 - \mathbb{E}_{\phi_k} \left[\exp \left[-\lambda_e \int_{\mathbb{R}^2} \Pr(\text{SINR}_k^e > \Gamma_e) de \right] \right], \end{aligned}$$

where (b) gives the upper bound on (a) by using independence of fading at each eavesdropper and generating functional of PPP.

The total secrecy outage probability, P_{so} , for the three tier network is defined as

$$P_{so} = \sum_{k=1}^3 P_{so}^k A_k. \quad (4.25)$$

The conditional secrecy outage probability for a typical user associated with

sub-6GHz MBS is given as,

$$P_{so}^1(\Gamma_e) = 1 - \exp\left(-2\pi\lambda_e \sum_{i=1}^N \binom{N}{i} (-1)^{i+1} \times \int_0^\infty r_e \exp\left[-\frac{i\Gamma_e r_e^{\alpha_1} \sigma^2}{\hat{P}_1} - \zeta_1^1 - \zeta_2^1\right] dr_e\right), \quad (4.26)$$

where $\hat{P}_1 = \frac{P_1}{S}$ and ζ_1^1 and ζ_2^1 is the characterization of interference from sub-6GHz MBSs and small cell BSs given as,

$$\zeta_1^1 = 2\pi\lambda_1 \sum_{\mu=1}^S \binom{S}{\mu} \int_{r_e}^\infty \frac{(u\hat{P}_1 r^{-\alpha_1})^\mu}{(1 + u\hat{P}_1 r^{-\alpha_1})^S} r dr,$$

$$\zeta_2^1 = 2\pi\lambda_2 \int_{\left(\frac{P_2}{(N-S+1)\hat{P}_1}\right)^{\frac{1}{\alpha_2}} r_e}^\infty \left(\frac{uP_2 r^{-\alpha_2}}{1 + uP_2 r^{-\alpha_2}}\right) r dr,$$

respectively, where $u = \left(\frac{i\Gamma_e r_e^{\alpha_1}}{\hat{P}_1}\right)$. Similarly, the conditional secrecy outage probability for a typical user associated with sub-6GHz small cell BS is given as

$$P_{so}^2(\Gamma_e) = 1 - \exp\left(-2\pi\lambda_e \int_0^\infty r_e \exp\left[-\frac{\Gamma_e r_e^{\alpha_2} \sigma^2}{P_2} - \zeta_1^2 - \zeta_2^2\right] dr_e\right), \quad (4.27)$$

where

$$\zeta_1^2 = 2\pi\lambda_1 \sum_{\mu=1}^S \binom{S}{\mu} \int_{\left(\frac{N-S+1}{P_2}\hat{P}_1\right)^{\frac{1}{\alpha_1}} r_e}^\infty \frac{(u\hat{P}_1 r^{-\alpha_1})^\mu}{(1 + u\hat{P}_1 r^{-\alpha_1})^S} r dr,$$

$$\zeta_2^2 = 2\pi\lambda_2 \int_{r_e}^\infty \left(\frac{uP_2 r^{-\alpha_2}}{1 + uP_2 r^{-\alpha_2}}\right) r dr,$$

where $u = \left(\frac{\Gamma_e r_e^{\alpha_2}}{P_2}\right)$. The conditional secrecy outage probability for a typical

user associated with mmWave small cell BS is given as,

$$P_{so}^3(\Gamma_e) = 1 - \exp\left(-2\pi\lambda_e \sum_{j \in \{L, N\}} \sum_{i=1}^{N_j} \binom{N_j}{i} (-1)^{i+1} \times \int_0^\infty r_e \exp\left[-\frac{i\Gamma_e r_e^{\alpha_j} \sigma^2}{P_3 G_e} - \zeta_{3,j}\right] p_j(r_e) dr_e\right), \quad (4.28)$$

where $p_L(r_e) = e^{(-\beta r_e)}$, $p_N(r_e) = 1 - e^{(-\beta r_e)}$, $\zeta_{3,L} = C_i(\Gamma_e, r_e) + D_i(\Gamma_e, r_e)$ and $\zeta_{3,N} = E_i(\Gamma_e, r_e) + V_i(\Gamma_e, r_e)$ respectively.

4.3 Simulation and Numerical Results

In this section, we validate the system model by taking a 3-tier HetNet with MBS density $\lambda_1 = (500^2 \times \pi)^{-1}$, where λ_2 and λ_3 are taken as multiples of MBS density. The sub-6GHz tiers are assumed to be operating at 1GHz carrier frequency, 10MHz bandwidth, path loss exponents $\alpha_1 = 3.5$, $\alpha_2 = 4$ and transmit power $P_1 = 46\text{dBm}$ and $P_2 = 30\text{dBm}$, respectively. The density of eavesdropper is taken as $\lambda_e = 1 \times 10^{-6}$. For mmWave tier, the operating frequency is 28GHz, 100MHz bandwidth, path loss exponent for LoS $\alpha_L = 2$ and for NLoS $\alpha_N = 4$ and transmit power $P_3 = 30\text{dBm}$. Nakagami fading parameters for mmWave tier, N_N and N_L , are taken 2 and 3, respectively. Array gains for all angles in main lobe are taken $M_r = 10\text{dB}$ and $M_t = 10\text{dB}$ and for the side lobes $m_r = -10\text{dB}$ and $m_t = 0\text{dB}$. Main lobe beamwidth is taken to be $\theta_r = 90^\circ$ and $\theta_t = 30^\circ$. Noise $\sigma^2 = -90\text{dBm}$ is taken with noise figure of 10dB. Blockage parameter, β , is $1/\beta = 141.4$ meters [22].

Fig. 4.1 shows the relationship between the association probability and varying mmWave BS density λ_3 and it is observed that the mmWave association increases with λ_3 . This is due to the fact that with increasing density, the

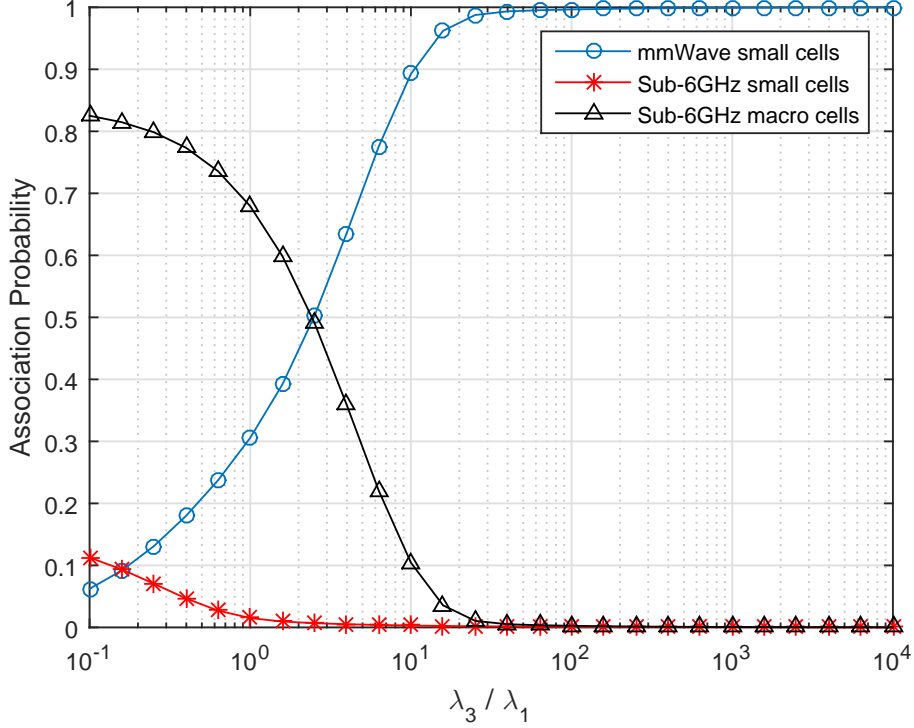


Figure 4.1: Association probability versus varying relative small mmWave BS density λ_3/λ_1 for $\lambda_2 = 30\lambda_1$, $N = 100$ and $S = 5$

average cell radius of the mmWave small cells decreases leading to stronger links between the user and mmWave BSs. Moreover, since LoS probability function, $p(R)$, is function of distance so when the distance decreases, the LoS association probability increases that increases the probability of the user to form lower path loss LoS links with mmWave BSs than the high path loss NLoS links. Though macro BSs have higher transmit power and large array gains, association with macro BSs decreases because of low BS density.

In Fig. 4.2 we can see the variation in secrecy outage probability versus SINR threshold at the eavesdropper for different eavesdropper antenna gains for mmWave tier and it is observed that secrecy outage probability falls with

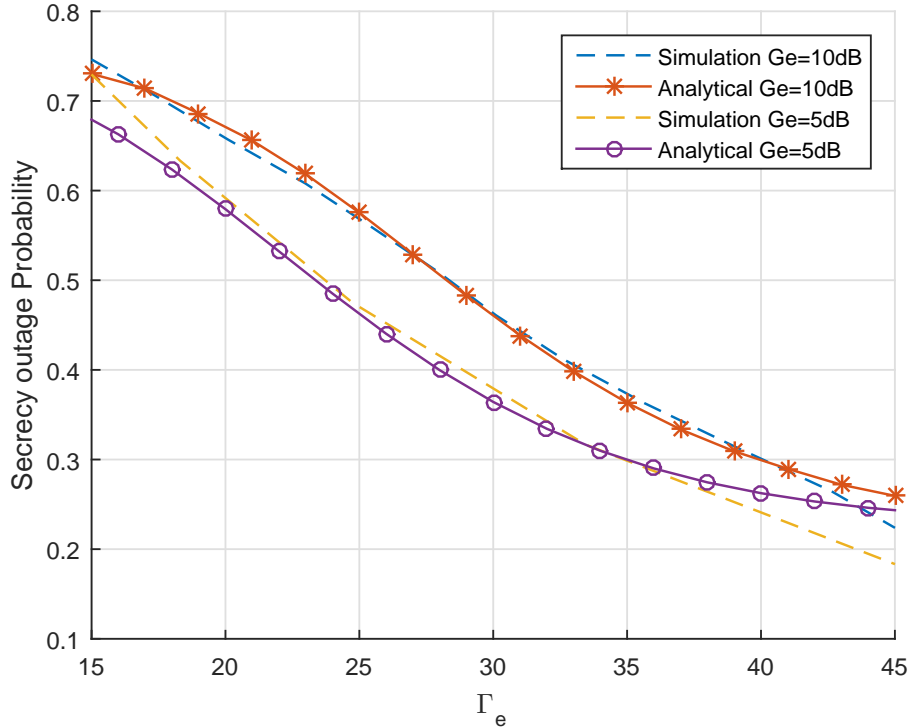


Figure 4.2: Secrecy outage probability versus Γ_e (dB) for $\lambda_2 = \lambda_3 = 30\lambda_1$, $N = 5$

increase in Γ_e and higher directivity gains lead to increased secrecy outage. Highly directional beamforming at mmWave tier leads to lower connection outage probability but since eavesdroppers too will have higher gains, there is a greater probability of them having SINR greater than threshold and thus transmission secrecy is compromised. Thus, there exists a tradeoff and it is not possible to set highly directional beams at mmWave BSs to improve connection outage while ignoring secrecy outage. Moreover, analytical results have been validated by Monte Carlo simulations.

Fig. 4.3 shows the behavior of secrecy outage probability as the density of eavesdropper is varied for different small cell BS densities and directional antenna gains at the eavesdroppers. It is observed that higher small cell BS

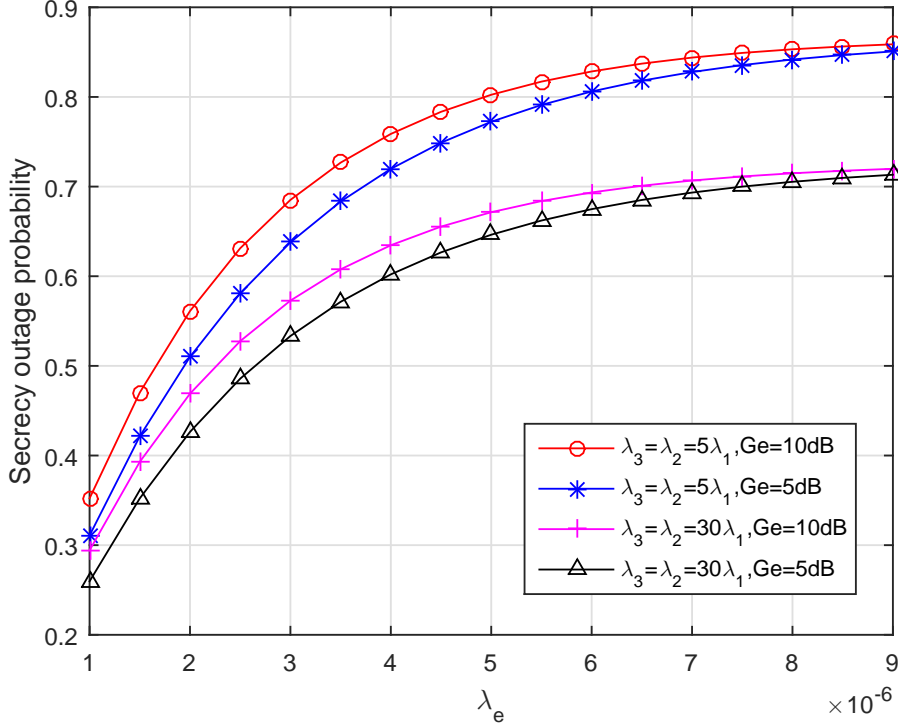


Figure 4.3: Secrecy outage probability as the function of λ_e for $\Gamma_e = 40\text{dB}$, $N = 5$

density improves the secrecy of the network as higher density yields greater overall network interference that leads to uncertainty at the eavesdropper and its SINR falls below the threshold. Moreover it is observed that keeping small cell density fixed, lower directional antenna gains at the eavesdroppers improves the secrecy capacity of the network transmissions. Thus lower directional gain and increased interference collectively decrease the chance of eavesdroppers SINR being above threshold.

Fig. 4.4 shows the secrecy outage probability variation with Γ_e for different number of antennas at macro BSs and it is observed that as the number of antennas at MBSs increases, the secrecy outage probability also increases. This is due to the fact that MBSs are higher power nodes as compared to

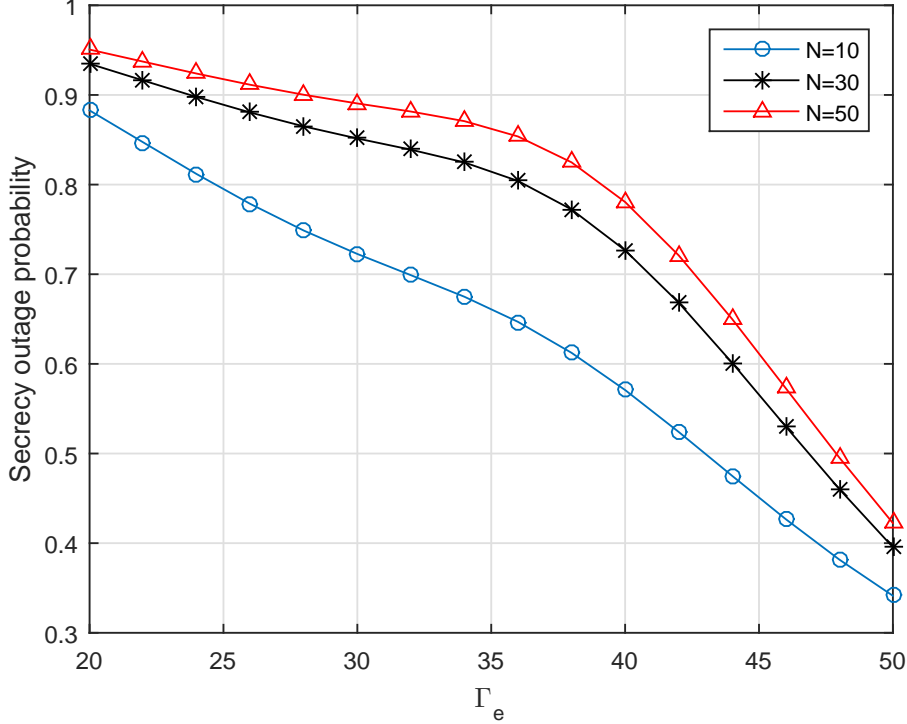


Figure 4.4: Secrecy outage probability versus Γ_e (dB) for $G_e = 15$ dB, $\lambda_2 = \lambda_3 = 30\lambda_1$

small cell BSs that leads to better transmission at legitimate as well as eavesdroppers nodes thus eavesdroppers are more likely to have SINR well above threshold. Moreover, when MBSs have higher antenna density, they provide higher array gains and users are less likely to be offloaded to small cells, therefore, overall interference of the network drops, leading to less uncertainty at the eavesdroppers. It can be observed from the figure that there is no substantial increase in secrecy outage after the number of antennas is increased beyond certain limit because after that user association with tiers does not have significant variation.

Fig. 4.5 shows the trend of EE and rate coverage probability versus SINR threshold Γ and achievable rate threshold ρ for different small cell BSs

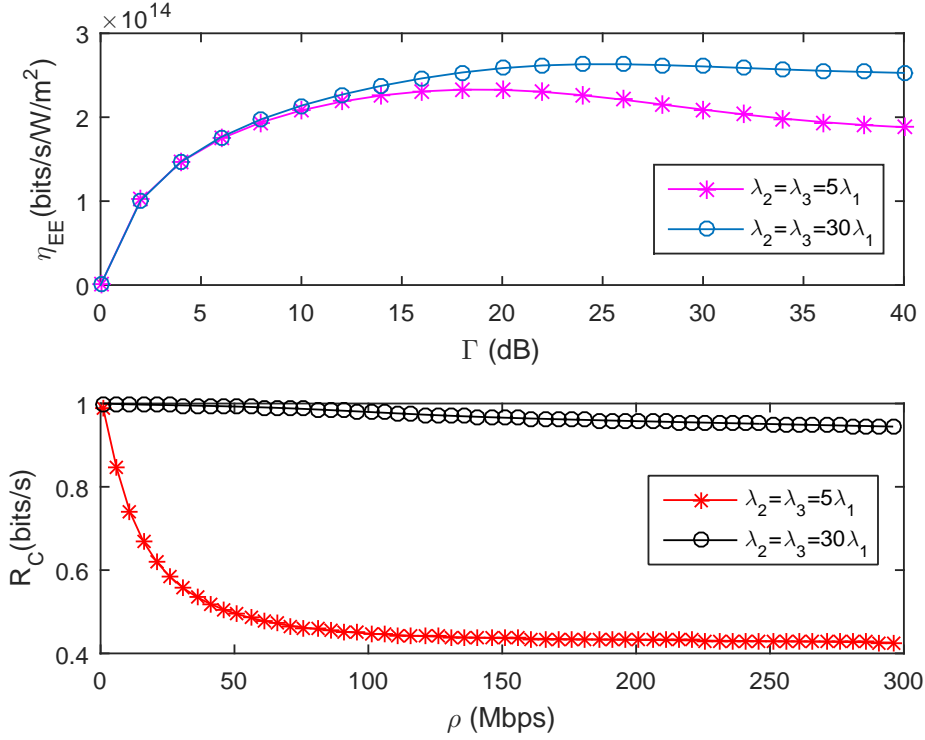


Figure 4.5: EE versus SINR threshold Γ and rate coverage probability versus achievable rate in Mbps ρ for $N = 4$, $S = 2$, $\lambda_u = 1 \times 10^{-4}$, $\epsilon = 0.9$ and $\rho_c = 0.1W$

density. It is observed that increasing the SINR requirement results in an increasing EE and outage probability. The trend is explained by (4.11) which outlines the dependence of EE on the coverage probability of the network and the SINR threshold. The EE increases with the term $\log_2(1 + \Gamma)$ since all other factors such as BS densities and number of antennas at MBSs are fixed. Rate trend shows that the rate of the network increases rapidly with the increase in small cell BS density. This is because with increased small cell BS density more users are offloaded to small cells and form better links. Moreover, users associated with mmwave small cells have higher allocated bandwidth.

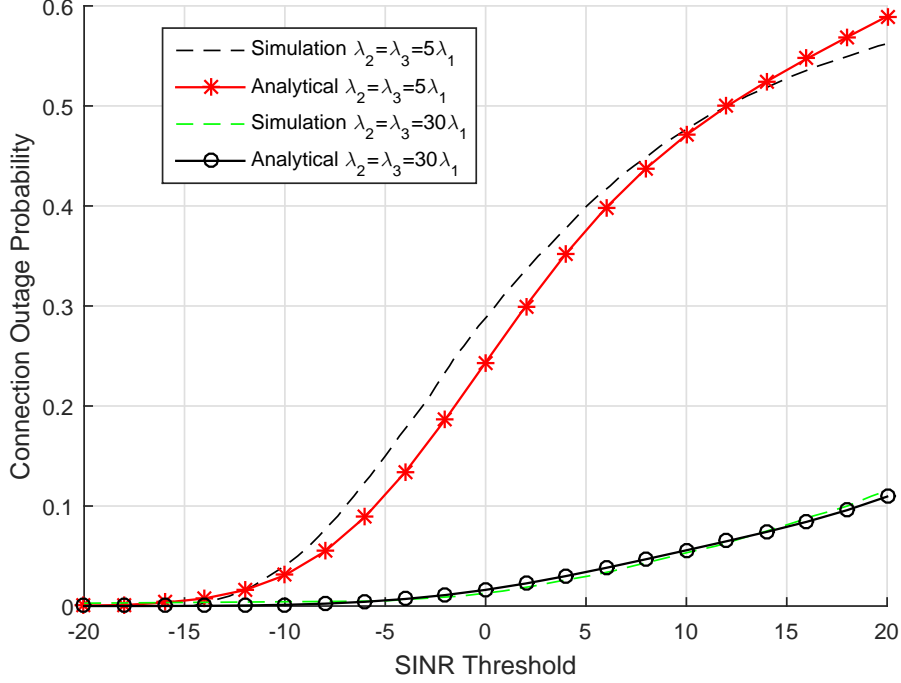


Figure 4.6: Connection outage probability versus SINR threshold Γ (dB) for $N = 4$ and $S = 2$

Fig. 4.6 shows the connection outage probability for different small cell BS densities and we observe that as small cell BS density increases, more users are offloaded to small cells and it significantly decreases the connection outage probability of the network. As small cells BSs are lower power nodes, this may lead to power efficient network where high power macro BS have lower traffic and density but it comes at the cost of high small cell BS deployment density. Moreover, analytical model is validated by simulations.

Fig. 4.7 shows the trend of EE and ASE verses SINR threshold for different small cell BSs density. It is observed that increasing the SINR requirement results in an increasing EE and ASE and their trends are almost similar. The trend is explained by (10) and (11) which outlines the depen-

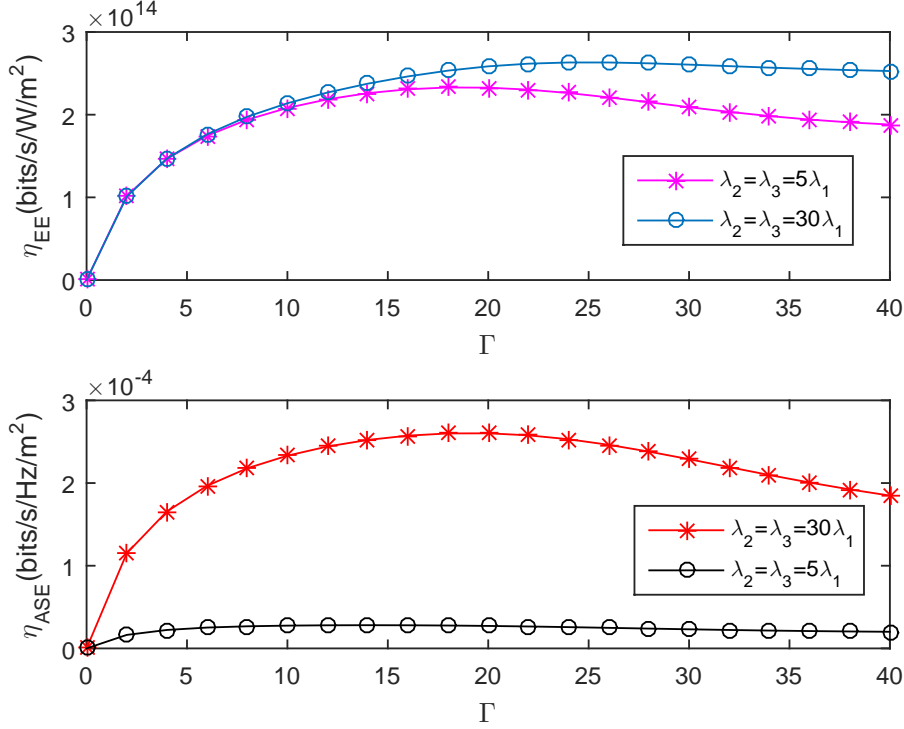


Figure 4.7: EE and SE versus SINR threshold Γ (dB) for $N = 4$, $S = 2$, $\lambda_u = 1 \times 10^{-4}$, $\epsilon = 0.9$ and $\rho_c = 0.1W$

dence of ASE and EE on the coverage probability of the network and the SINR threshold. The EE and ASE increase with the term $\log_2(1 + \Gamma)$ since all other factors such as BS densities and number of antennas at MBSs are fixed. However, at larger SINR thresholds, the increase in connection outage probability becomes dominant and as a result, the ASE decreases.

Fig. 4.8 shows the connection outage probability comparison of 2-tier network with sub-6GHz macro and small cells and 3-tier network with mmWave small cells and we observe that the mmWave tier has a major role in keeping outage event low. This can be attributed to the larger available bandwidth, higher density and favourable SINR distribution of mmWave cells. Macro cells may serve to decrease service outage at cell edges but within them small

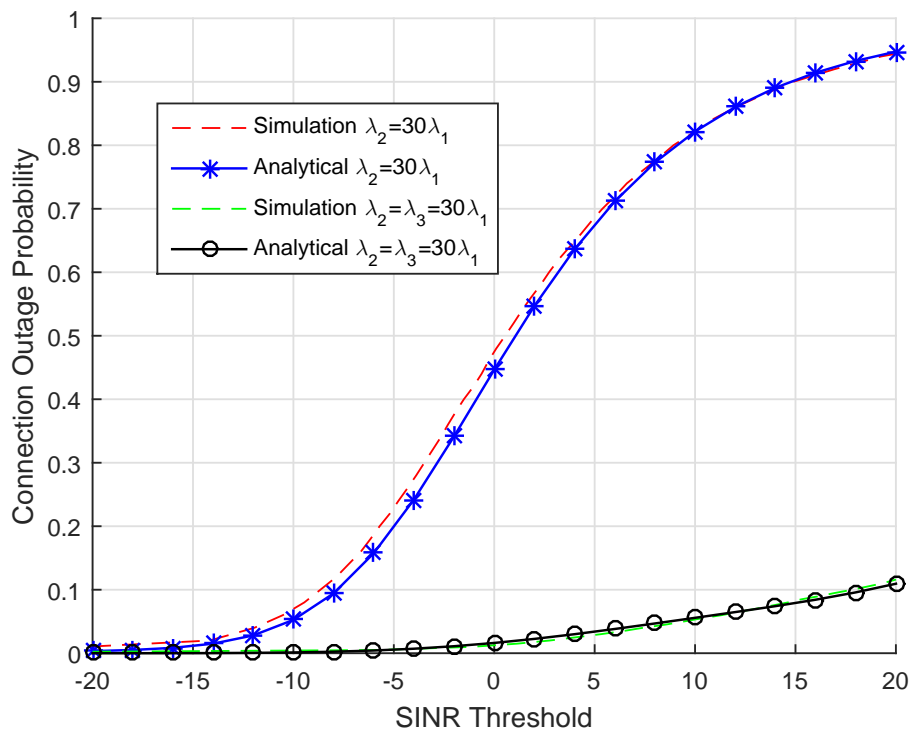


Figure 4.8: Connection outage probability versus SINR threshold Γ for $N = 4$ and $S = 2$

cells serve the purpose. Moreover, analytical model is validated by simulations.

Chapter 5

Conclusions and Future Works

In this thesis, we modeled and analyzed various enabling technologies for 5G cellular networks. This work analyzed and presented valuable results for enhancing the performance of HetNets by complementing them with massive MIMO and mmWave technologies. We conclude the thesis in two parts

- In Chapter 3, 3-tier HetNet coverage and rate is analysed with massive MIMO at macro tier. User association is performed based on maximum received power and effect of massive MIMO and mmWave BS density on the user cell association is investigated. It has been observed that the implementation of massive MIMO on macro tier and deployment of high density of mmWave small cells leads to significant enhancement of rate and coverage. Moreover, numerical results showed that on increasing number of antennas at macro BS, user association is biased towards macro tier, leading to low demand of small cells that simplifies the network.
- In Chapter 4, we investigate the impact of massive MIMO and mmWave small cells on the connection and secrecy outage probability, ASE and

EE of a 3-tier heterogeneous network. User association with BS is based on maximum average received power. Association probability for fixed number of antennas at the MBSs is biased towards mmWave small cells. It has been observed that higher density of sub-6GHz and mmWave small cells leads to considerable decrease in connection outage and secrecy outage probability and significant enhancement of ASE and EE of the network. Moreover, it is critical to mention that directivity gains for mmWave BSs and number of antennas at MBSs cannot be increased limitlessly to offload traffic to small cells and decrease network outage capacity since that elevates the secrecy outage capacity, i.e., there exist a tradeoff between secrecy outage and connection outage probability. Since small cells BSs are lower power nodes, this leads to a power efficient network but it comes at the cost of their higher deployment density.

The possible future works based on this thesis are the modeling and performance analysis of the presented 3 tier hybrid heterogeneous network by introduction of dual slope model at the millimeter wave tier. Because of the propagation losses associated with millimeter wave technology it is desirable to follow multi slope path loss models at millimeter wave tier.

It will be worthwhile to evaluate of the performance of proposed framework based on various optimization theories to optimize its energy efficiency and area spectral efficiency by minimizing the transmitted power per base station and also by minimizing the density of small cell base stations because of their hardware cost.

As far the secrecy analysis is concerned, the modeling and performance analysis of proposed 3 tier hybrid heterogeneous framework in terms of se-

crecy outage and connection outage for the artificial noise addition scheme for secrecy will be a worthwhile contribution to 5G.

Bibliography

- [1] Cisco, “Cisco visual networking index: Global mobile data traffic forecast update, 2012-2017,” *Whitepaper* available at: <http://goo.gl/xxLT>.
- [2] Q. Ye, B. Rong, Y. Chen, M. Al-Shalash, C. Caramanis, and J. G. Andrews, “User association for load balancing in heterogeneous cellular networks,” *IEEE Trans. on Wireless Commun.*, vol. 12, no. 6, pp. 2706-2716, 2013.
- [3] Hu, R. Q., Qian, Y., Kota, S., Giambene, G., “HetNets - A New Paradigm for Increasing Cellular Capacity and Coverage [Guest Editorial]” *IEEE Wireless Communications*, vol. 18, no. 3, pp. 8-9, June 2011.
- [4] A. Umer, S. A. Hassan, H. B. Parveiz, L. Musavian, Q. Ni, “Coverage and Rate Analysis for Massive MIMO enabled Heterogeneous Networks with Millimeter wave Small Cells”, *Proceedings of the IEEE Vehicular Technology Conference (VTC-Spring)*, Jun, 2017.
- [5] A. Damnjanovic, J. Montojo, Y. Wei, T. Ji, T. Luo, M. Vajapeyam, T. Yoo, O. Song and D. Malladi, “A survey on 3GPP heterogeneous networks,” *IEEE Wireless Communications*, vol. 18, no. 3, pp. 10-21, 2011.

- [6] A. Ghosh, N. Mangalvedhe, R. Ratasuk, B. Mondal, M. Cudak, E. Visotsky, T. A. Thomas, J. G. Andrews, P. Xia, H. S. Joet al., “Heterogeneous cellular networks: From theory to practice,” *IEEE Communications Magazine*, vol. 50, no. 6, pp. 54-64, 2012.
- [7] D. Lopez-Perez, I. Guvenc, G. De la Roche, M. Kountouris, T. Q. Quek, and J. Zhang, “Intercell interference coordination challenges in heterogeneous networks,” *IEEE Wireless Commun.*, vol. 18, no. 3, pp. 22-30, 2011.
- [8] S. W. Hasan and S. A. Hassan, “Fuzzy Logic-based Downlink Subchannel Allocation for Capacity Maximization in OFDMA Femtocells,” *IEEE International Wireless Communications and Mobile Computing Conference (IWCMC)*, Aug, 2015.
- [9] R. Zahid and S. A. Hassan, “Stochastic Geometry-based Analysis of Multiple Region Reverse Frequency Allocation Scheme in Downlink Het-Nets”, *IEEE International Wireless Communications and Mobile Computing Conference (IWCMC)*, Aug, 2015, Croatia.
- [10] H. Pervaiz, L. Musavian, and Q. Ni, “Energy and spectrum efficiency trade-off for Green Small Cell Networks,” *IEEE International Conf. on Commun. (ICC)*, pp. 5410-5415, 2015.
- [11] J. Liu, D. Wang, J. Wang, J. Li, J. Pang, G. Shen, Q. Jiang, H. Sun and Y. Meng, “Uplink power control and interference coordination for heterogeneous network,” *IEEE International Symposium on Personal Indoor and Mobile Radio Communications (PIMRC)*, pp. 519-523, 2012.

- [12] F. Baccelli H. S. Dhillon, R. K. Ganti and J. G. Andrews, “Modeling and analysis of k-tier downlink heterogeneous cellular networks,” *IEEE J. Sel. Areas Commun.*, vol. 30, no. 3, pp. 550U560, April 2012.
- [13] M. S. Omar, M. A. Anjum, S. A. Hassan, H. Pervaiz and Q. Ni, “Performance analysis of hybrid 5G cellular networks exploiting mmWave capabilities in suburban areas,” *IEEE Int. Conf. Commun. (ICC)*, pp. 1-6, 2016.
- [14] H. C. Papadopoulos D. Bethanabhotla, O. Y. Bursalioglu and G. Caire, “Optimal user-cell association for massive mimo wireless networks,” <http://arxiv.org/abs/1407.6731>, 2014.
- [15] Yue Chen Maged ElKashlan Anqi He, Lifeng Wang and Kai-Kit Wong, “Massive mimo in k-tier heterogeneous cellular networks: Coverage and rate,” *10.1109/GLOCOM.2014.7417732*, Dec.2015.
- [16] M. Kountouris Y. S. Soh, T. Q. S. Quek and H. Shin, “Energy efficient heterogeneous cellular networks,” *IEEE J. Sel. Areas Commun.*, vol. 31, no. 5, pp. 840U850, May 2013.
- [17] T. Han Q. Li X. Ge, S. Tu and G. Mao, “Energy efficiency of small cell backhaul networks based on gauss-markov mobile models,” *IET Networks*, Vol. 4, No. 2, pp. 158-167, 2015.
- [18] J. Ye G. Mao C.X. Wang X. Ge, B. Yang and T. Han, “Spatial spectrum and energy efficiency analysis of random cellular networks,” *IEEE Trans. on Commun.*, Vol. 63, No. 3, pp. 1019-1030, 2015.

- [19] S. Vuppala and G. T. F. de Abreu, "Unicasting on the secrecy graph," *IEEE Trans. Inf. Forensics Security*, vol. 8, no. 9, pp. 1469-1481, 2013.
- [20] P. K. Gopala, L. Lai, and H. El Gamal, "On the secrecy capacity of fading channels," *IEEE Trans. Inf. Theory*, vol. 54, no. 10, pp. 4687-4698, 2008.
- [21] Y. Liang, H. V. Poor, and S. Shamai, "Secure communication over fading channels," *IEEE Trans. Inf. Theory*, vol. 54, no. 6, pp. 2470-2492, 2008.
- [22] Tianyang Bai and Robert W. Heath, "Coverage and rate analysis for millimeter-wave cellular networks," *IEEE Transactions on Wireless Communications*, 1100-1114, 2015.
- [23] S.Vuppala, S.Biswas and T.Ratnarajah, "An Analysis on Secure Communication in Millimeter/Micro-Wave Hybrid Networks," *IEEE Trans. Commun.*, vol. 64, no. 8, pp. 3507-3519, 2016.
- [24] R. C. Daniels J. N. Murdock T. S. Rappaport, R. W. Heath Jr., "Millimeter Wave Wireless Communication," *Prentice Hall*, 2014.
- [25] S.Q. Xiao, M.T. Zhou and Y.Zhang, "Millimeter wave technology in wireless PAN, LAN, and MAN." *CRC Press*, 2008.
- [26] E. Ben-Dor J. N. Murdock Y. Qiao J. I. Tamir T. S. Rappaport, F. Gutierrez, "Broadband millimeter-wave propagation measurements and models using adaptive-beam antennas for outdoor urban cellular communications," *IEEE Trans. Antennas Propag.*, vol. 61, no. 4, pp. 1850-1859, Apr. 2013.

- [27] S. Rangan-E. Erkip M. R. Akdeniz, Y. Liu, “Millimeter wave picocellular system evaluation for urban deployments,” *Proc. Globecom Workshops (GC Wkshps)*, pp. 105U110, Dec. 2013.
- [28] E. Erkip S. Rangan, T. S. Rappaport, “Millimeter wave cellular wireless networks: Potentials and challenges,” *Proc. IEEE*, vol. 102, no. 3, pp. 366U385, Mar. 2014.
- [29] R. W. Heath T. Bai, R. Vaze, “Analysis of blockage effects on urban cellular networks,” *IEEE Trans. Wireless Commun*, vol. 13, no. 9, pp. 5070U5083, Sept. 2014.
- [30] E. G. Larsson H. Q. Ngo and T. L. Marzetta, “The multicell multiuser mimo uplink with very large antenna arrays and a finite-dimensional channel,” *IEEE Trans. Commun.*, vol. 61, no. 6, pp. 2350U2361, June, 2013.
- [31] W. Yu K. Hosseini and R. S. Adve, “Large-scale mimo versus network mimo for multicell interference mitigation,” *IEEE J. Sel. Areas Commun*, vol. 8, no. 5, pp. 930U941, Oct. 2014.
- [32] M. ElKashlan-Trung Q. Duong L. Wang, H. Q. Ngo and K. K. Wong, “Massive mimo in spectrum sharing networks: Achievable rate and power efficiency,” *IEEE Systems Journal*, pp. 1-12, 2015.
- [33] A. M. Tulino H. Huh and G. Caire, “Network mimo with linear zeroforcing beamforming: Large system analysis, impact of channel estimation, and reduced-complexity scheduling,” *IEEE Trans. Inf. Theory*, vol. 58, no. 5, pp. 2911U2934, May 2012.

- [34] X. Ge, T. Han, Y. Zhang *et al.*, “Spectrum and energy efficiency evaluation of two-tier femtocell networks with partially open channels,” *IEEE Trans. Vehicular Tech.*, vol. 63, no. 3, pp. 1306-1319, 2014.
- [35] D. Satyanarayana and J. M. Elmirghani, “An energy efficient network architecture for infrastructured wireless networks,” *Proc. IEEE Global Telecommun. Conf. (GLOBECOM)*, pp 1-6, 2010.
- [36] V. Jungnickel *et al.*, “The role of small cells, coordinated multipoint, and massive MIMO in 5G,” *IEEE Commun. Mag.*, vol. 52, no. 5, pp. 44-51, 2014.
- [37] T. L. Marzetta, “Noncooperative cellular wireless with unlimited numbers of base station antennas,” *IEEE Trans. Wireless Commun.*, vol. 9, no. 11, pp. 3590-3600, Nov. 2010.
- [38] M. ElKashlan-Trung Q. Duong L. Wang, H. Q. Ngo and K. K. Wong, “Massive mimo in spectrum sharing networks: Achievable rate and power efficiency,” *IEEE Systems Journal*, pp. 1-12, 2015.
- [39] E. Erkip S. Rangan, T. S. Rappaport, “Millimeter wave cellular wireless networks: Potentials and challenges,” *Proc. IEEE*, vol. 102, no. 3, pp. 366-385, 2014.
- [40] S. Rangan-E. Erkip M. R. Akdeniz, Y. Liu, “Millimeter wave picocellular system evaluation for urban deployments,” *Proc. Globecom Workshops (GC Wkshps)*, pp. 105-110, Dec. 2013.
- [41] H. Munir, S. A. Hassan, H. B Parveiz, L. Musavian, Q. Ni, “Resource Optimization in Multi-Tier HetNets Exploiting Multi-Slope Path Loss Model”, *IEEE Access*, May, 2017.

- [42] A. Ijaz, S. A. Hassan, S. A. R. Zaidi, D. N. K. Jayakody, , “Coverage and Rate Analysis for Downlink HetNets Using Modified Reverse Frequency Allocation Scheme”, *IEEE Access*, Feb, 2017.
- [43] Muhammad Shahmeer Omar, Syed Ahsan Raza Naqvi, Shahroze Humayun Kabir, Syed Ali Hassan, “An Experimental Evaluation of a Cooperative Communication-based Smart Metering Data Acquisition System”, *IEEE Transactions on Industrial Informatics*, vol. 13, no. 1, pp. 399-408, Feb 2017.
- [44] H. Munir, S. A. Hassan, H. B. Parveiz, Qiang Ni, L. Musavian, “User Association in 5G Heterogeneous Networks Exploiting Multi-Slope Path Loss Model”, *IEEE Second Workshop on Recent Trends in Telecommunications Research*, Feb. 2017.
- [45] A. Ijaz, S. A. Hassan and D. N. K. Jayakody, “A Multiple Region Reverse Frequency Allocation Scheme for Downlink Capacity Enhancement in 5G HetNets,” *IEEE Consumer Communications and Networking Conference (CCNC)*, Jan. 2017.
- [46] Soma Qureshi, S. A. Hassan, N. K. Jayakody, “Successive Bandwidth Division NOMA Systems: Uplink Power Allocation with Proportional Fairness”, *Proceedings of the IEEE Consumer Communications and Networking Conference (CCNC)*, Jan, 2016.
- [47] H. Munir, S. A. Hassan, H. B. Parveiz, Leila Musavian, Qiang Ni, “Energy Efficient Resource Allocation in 5G Hybrid Heterogeneous Networks: A Game Theoretic Approach”, *Proceedings of the IEEE Vehicular Technology Conference (VTC-Fall)*, Sep, 2016.

- [48] M. S. Omar, S. A. Raza, M. S. Humayun, S. A. Hassan, “Analysis of Cooperative Transmissions as an Enabling Technology for Smart Grid Data Aggregation: An Experimental Perspective”, *IEEE Conference on Industrial Informatics*, July 2016.
- [49] M. S. Omar, M. A. Anjum, S. A. Hassan, H. Parveiz, Q. Ni, “Performance Analysis of Hybrid 5G Cellular Networks Exploiting mmWave Capabilities in Suburban Areas”, *IEEE International Conference on Communications (ICC)*, May, 2016.
- [50] H. Munir, S. A. Hassan, H. Parveiz, Q. Ni, “A Game Theoretical Network-Assisted User-Centric Design for Resource Allocation in 5G Heterogeneous Networks”, *IEEE Vehicular Technology Conference (VTC-Spring)*, May, 2016.
- [51] S. A. R. Naqvi, S. A. Hassan, Z. Mulk, “Pilot Reuse and Sum Rate Analysis of mmWave and UHF-based Massive MIMO Systems”, *Proceedings of the IEEE Vehicular Technology Conference (VTC-Spring)*, May, 2016.
- [52] S. Qureshi and S. A. Hassan, “MIMO Uplink NOMA with Successive Bandwidth Division”, *IEEE Wireless Communications and Networking Conference (WCNC)*, April 2016.
- [53] M. S. Omar, S. A. Raza, S. H. Kabir, M. Hussain, S. A. Hassan, “Experimental Implementation of Cooperative Transmission Range Extension in Indoor Environments”, *IEEE International Wireless Communications and Mobile Computing Conference (IWCMC)*, Aug, 2015.